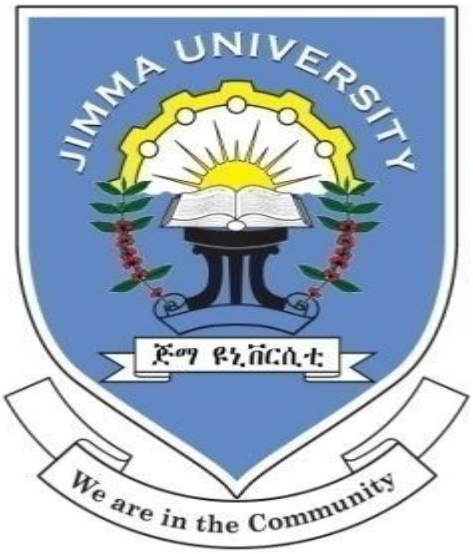

JIMMA UNIVERSITY

SCHOOL OF GRADUATE STUDIES

JIMMA INSTITUTE OF TECHNOLOGY

FACULTY OF CIVIL AND ENVIRONMENTAL ENGINEERING

STRUCTURAL ENGINEERING STREAM

PARTIALLY ENCASED COMPOSITE COLUMN RESPONSE USING DIFFERENT TYPES OF PLATE THICKNESS AND TRANSVERSE LINK UNDER AXIAL LOAD

A Research Submitted to the School of Graduate Studies of Jimma University in Partial Fulfillment of the Requirements for the Degree of Master of Science in Structural Engineering

By: Robe Kudama

July 2021

Jimma, Ethiopia

JIMMA UNIVERSITY

SCHOOL OF GRADUATE STUDIES

JIMMA INSTITUTE OF TECHNOLOGY

FACULTY OF CIVIL AND ENVIRONMENTAL ENGINEERING

STRUCTURAL ENGINEERING STREAM

PARTIALLY ENCASED COMPOSITE COLUMN RESPONSE USING DIFFERENT TYPES OF PLATE THICKNESS AND TRANSVERSE LINK UNDER AXIAL LOAD

A Research submitted to the School of Graduate Studies of Jimma University in Partial Fulfillment of the Requirements for the Degree of Master of Science in Structural Engineering

By: Robe Kudama

Engr. Elmer C. Agon(Asso. Prof)

Main advisor

Engr. Menbaru Elias(Msc)

Co-advisor

July 2021

Jimma, Ethiopia

DECLARATION

This thesis research is my original work and has not been presented for a Master's of Degree in any other University. All sources used in this thesis are duly acknowledged.

_____	_____	_____
Name	Signature	Date

This thesis work has been submitted for examination with my approval as university supervisor.

_____	_____	_____
Advisor’s Name	Signature	Date
_____	_____	_____
Co-Advisor’s Name	Signature	Date
_____	_____	_____
Examiner's Name	Signature	Date

Abstract

There are two types of composite columns, concrete encased section, and concrete-filled steel tube which are commonly used in buildings. Concrete Encased Steel (CES) composite columns have been of interest to many researchers due to their excellent structural performance under both static and seismic loading conditions.

Concrete encased steel (CES) composite columns can be divided into two categories: Fully Encased Composite (FEC) column and Partially Encased Composite (PEC) column. This study focused on the PEC column response by using different types of plate thickness and transverse link under axial load. In partially encased composite column, the steel flange is not externally restrained by the concrete so, it may deform outwards. The analysis was performed by the finite element analysis (FEA) software package ABAQUS 6.14. The geometric parameters for the study were the thickness of H-section, and transverse link arrangements. A parametric investigation procedure was done on a series of fourteen (14) samples column. The study considered H-section with a thickness of web (from 7.2mm to12.7mm), thickness of flanges (from 11mm to 20.5mm), and link shapes (horizontal, X-shape, and Z-shape).

The result from the study shows the capacity of partially encased composite column increase with the decrease of effective width to the thickness of flange (b/T) or effective width to thickness of web (b/t). The peak capacity of C-5 specimen is 38.37 *% higher than the peak capacity of C-1 specimen when the b/T ratio decreased from 9.5 to 5.1. As the b/t ratio is reduced from 14.5 to 8.2 the axial load capacity of PEC columns was increased by 32 %.*

The transverse link increases the axial capacity of the partially encased composite (PEC) column. From three types of link arrangement X-shape link has 38.72 % and 16.75% higher peak load capacity than horizontal and Z-shape link respectively.

Keywords: *FEA, Thickness, Link arrangement, PEC column, Axial load.*

Acknowledgment

First and at most, greatest thanks from the depth of my heart is to Almighty GOD for endowing me with the courage, strength as well as health throughout my school time and the full support provided by him for the successful accomplishment of my MSc class and preparation of this MSc thesis.

My deepest gratitude goes to my advisor **Mr. Elmer C Agon (Associate Professor)** and my co-advisor **Eng. Menbaru Elias (MSc)** for all their limitless efforts in guiding me through my work and appreciation of my efforts and for providing me useful reference material needed to achieve my goal. I would like to extend my thanks and appreciation to Jimma University, School of Graduate Studies, Jimma Institute of Technology, Civil and Environmental Engineering Department, Structural Engineering chair holder, and all academic staff of a civil engineering department, librarians, and administrative workers of the Institute.

Next, I would like to say thanks a lot to all my friends who shared their unselfish help and kind support in preparing this thesis. Finally, my special thanks go to my parents who are always been there in times of difficulties, and for giving me moral support.

Table of Contents

List of Table

List of Figure

Acronyms and Abbreviations

CES	Concrete-Encased Steel
CFRC	Concrete Filled Rectangular Column
CFST	Concrete Filled Steel Tube
EC	European Code
ESEN	Ethiopian Standards Based On European Norm
FEC	Fully Encased Composite
FEC	Fully Encased Composite
FEM	Finite Element Method
FRP	Fiber Reinforcement Polymer
RC	Reinforced Concrete
PEC	Partially Encased Composite
HSC	High Strength concrete
NSC	Normal Strength Concrete
FE	Finite Element
DOF	Degree of Freedom
CDP	Concrete Damage Plasticity
CFST	Concrete Filled Steel Tube

3D	Three Dimensional
C3D8R	8-Node Linear Brick, Reduced Integration, Hourglass
S	Spacing
B	Effective Width of Flange
D	Effective Depth of Cross-Section
T	Thickness of Web
T	Thickness of Flange
T3d2	2-Node Linear 3-D Truss
Fck	Compressive Strength of Concrete
Fy	Yield Strength of Steel

CHAPTER ONE

INTRODUCTION

1.1 Background of the study

Over the past several decades, the use of composite steel-concrete framing systems for buildings has gained popularity. The design of a framing system that combines structural steel and reinforced concrete produces a building having the advantages of each material, namely the inherent mass, stiffness, damping, and economy of reinforced concrete, and the speed of construction, strength, long-span capability, and lightweight of structural steel.

In recent decades, composite members are widely used by the designers in seismic zones because of their appropriate behavior in seismic motion (Ahmadi et al., 2017). There are two types of composite columns, those with a steel section encased in concrete and those with a steel section in-filled with concrete which is commonly used in buildings. Basic forms of cross-sections representative of composite columns are indicated in Figure1.

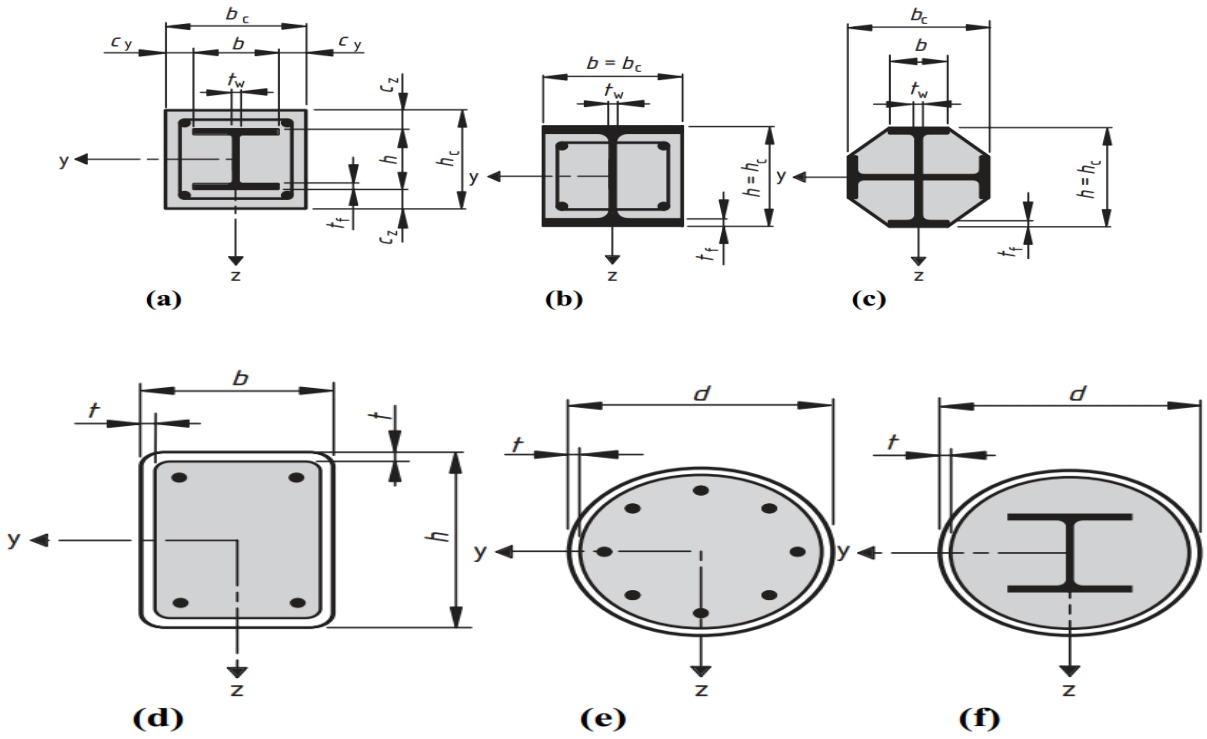

Figure 1.1 Typical cross-section of composite columns and notation (ES EN, 2015)

(a)Fully encased composite column (FEC), (b) partially encased composite column (PEC), (c) cruciform partially encased composite column, (d) concrete filled rectangular column (CFRC), (e) concrete filled steel tube (CFST), (f) steel-encased-concrete-filled-steel-tube column.

The concrete-encased composite structure is a typical kind of composite structure defined as a construction in which both steel and concrete materials are effectively combined to maximize the structural and economic advantages of each material. This type of construction is applied to high-rise buildings and metro railway stations to resist dynamic loads due to the movement of a train. Concrete-encased steel composite columns have become the preferred form of the structure due to their smaller sectional dimension, higher load-carrying capacity, and excellent structural performance under both static and seismic loading conditions when compared with reinforced concrete structures.

CES columns can be divided into two categories: Fully Encased Composite (FEC) column and Partially Encased Composite (PEC) column. FEC column generally has similar geometric configurations to conventional Reinforced Concrete (RC) column except for the presence of steel section, which can be H-shaped; cruciform shaped, and even consists of several steel sections depending on the specific structural requirement as shown in Figure 1. The Partially encased composite (PEC) members have been put into practice in past decades. Usually, these columns are made of an H-shaped plate, and spacing between web Partially encased composite (PEC) columns are one of the recent developments in the field of composite and flange is filled with normal-strength concrete.

The PEC member takes advantage of prefabrication, simple installation of formwork, efficient compressive load capacity, and fire resistance inherent in a concrete column In multi-story building structures, partially encased steel with a thinner plate can be advantageous for PEC members, with the advantage of further material saving, and structural weight reduction but, a thin plate with a large width-thickness ratio shall affect the structural behavior of PEC members (Chen, et al., 2010).

However, this study presented the behavior and strength of partially encased composite columns under axial compressive loading. This paper aim was to conduct a numerical study on the axial

compressive load performance of PEC by the finite element analysis software package ABAQUS 2014. These studies rather focus on the effectiveness of stiffener arrangement (shape) on improving the failure behavior, ductility, and toughness of the proposed columns.

1.2 Statement of the problem

A disadvantage of the steel element subjected to compression is that it is prone to buckling. As the length and slenderness ratio of compression members increased a buckling of the members' increases. For most structures, the use of composite columns is very economical due to their strength-to-weight ratios. But, additional steel is needed to stiff them so, they not buckle. When the PEC column is filled with concrete within steel flanges, only the web component is fully restrained by concrete encasement, whereas the flanges are susceptible to local buckling unless a certain requirement of width to thickness ratio is fulfilled. As listed in table 3, according to (ES EN 1993, 2015), all the PEC columns with H-section are categorized into Class 4 sections, while cruciform sections have either Class 1 or Class 3 steel sections. Most specimens with Class 4 steel sections cannot reach the EC4 predicted axial capacity, which means the load-carrying capacity of PEC columns may be restricted by the elastic local buckling of the slender steel section. However, in the case of the concrete-filled composite column, the axial resistance of concrete-filled sections is greater because the concrete is not able to expand laterally (Poisson's ratio effect) under load, and tri-axial stresses are developed in the concrete. This causes an increase in the compressive strength of the concrete by an amount dependent on the proportions of the cross-section. But in terms of PEC, the concrete is partially restrained by the steel section, and the unrestrained part of concrete able to expand outward and cause local buckling of the flange. So, additional strengthening techniques may be needed to overcome this effect.

More recently, experimental and analytical research was carried out on PEC columns subjected to eccentrically axial load or flexural load (Xianzhong Zhao, 2019) and (Begum, et al., 2007) Experimental investigation on the PEC column on the width-thickness ratio mainly focused on the flange of H- steel, by providing a transverse link between flanges which is parallel to the web of H-section was investigated (Chen, et al., 2010), et al, (Pereira, et al., 2015). The thinner plate had the merit of further material saving and structural weight reduction but, a thin plate with a

large width to thickness ratio is very sensitive to local buckling of the flange (Pereira, et al., 2015).

1.2 Research question

1. What are the effects of the effective width to thickness ratio (*b/T*) of a flange on the response of the PEC column subjected to axial compressive load?
2. What are the effects of the effective width to thickness ratio of the web (*b/t*) on the response of the PEC column subjected to axial compressive load?
3. What is the effect of the transverse link shape on the response of the PEC column?

1.4 Objectives of the study

1.4.1 General objective

The general objective of this study was to investigate the response PEC column using different types of thickness of plate and transverse link on the PEC column under axial loading.

1.4.2 Specific objective

The specific objectives of the study were:

1. To investigate the effects of width to thickness ratio of the flange (*b/T*) on the response of the PEC column
2. To investigate the effects of width to thickness of the web (*b/t*) on the response of the PEC column
3. To assess the impacts of the transverse link (stiffener) arrangements on the response of the PEC column

1.5 Significance of the study

Constructing buildings by composite structures get major importance throughout the World. Composite structures are cost-effective due to the spaces they provide. This study was conducted to investigate the response of partially encased composite columns by considering some parametric studies such as the thickness of the section, and stiffener shape. The study may help structural engineers to clearly understand the behavior and technique of strength of the partially encased composite column. The study may help to predict the axial capacity of PEC by considering the study parameters. Finally, the study will contribute significant input to other researchers for further study.

1.6 Scope of the study

The presented study is limited to the response of PEC using different steel structure thickness and reinforcement method. The scope was extended to cover the analysis by using FEM and it covers only the axial load carrying capacity, deformability, and failure modes of the partially encased composite column. The numerical analysis was done in nonlinear 3D finite element software ABAQUS 6.14 based on experimental validation. There is no experimental investigation conducted in this study.

CHAPTER TWO

REVIEW OF RELATED LITERATURE

Over the past several decades, the use of composite steel-concrete framing systems for buildings has gained popularity. The design of a framing system that combines structural steel and reinforced concrete produces a building having the advantages of each material, namely the inherent mass, stiffness, damping, and economy of reinforced concrete, and the speed of construction, strength, long-span capability, and lightweight of structural steel.

To increase the ductility of the column some reinforcing and construction methods have been reported, such as concrete in filled steel tube, confining RC columns by arranging transverse reinforcement as hoop ties closely and fully or partially encasing concrete-steel composite.

2.1 Concrete-encased composite column

2.1.1 Experimental investigation

Extensive experimental researches were carried out on encased composite columns, by several research groups to investigate the behavior and strength of encased composite columns under various loading conditions. A large number of tests were performed on short FEC columns constructed with normal strength concrete subjected to concentric, eccentric, and biaxial load. A few long column tests were carried out using normal strength concrete under static loading conditions. Findings of these experimental investigations are presented below:

Experimental investigation on the Behavior of Fully Encased Steel-Concrete Composite Columns Subjected to Monotonic and Cyclic loads was studied by (Cristina, et al., 2015) the study was conducted to investigate the behavior of FEC composite columns with high-strength concrete. Failure modes were different, characterized by sudden and violent concessions due to cracking developments through aggregate in columns with HSC, while columns with NSC show a “slow” failure mode characterized by the gradual decline of bearing capacity with the growth of the displacements. It is well known that high-strength concrete is more susceptible to fragile failure than normal concrete. On the other hand, from the graphics and parameters analysis, we can conclude that the columns with HSC have a higher energy absorption capacity, which can recommend this solution to the construction in seismic areas even the failure mode was brittle. In structural terms, composite columns with concrete class C70/85 provide obvious

better performances to structures, having significant increases to almost all analyzed parameters. The solution of a fully encased composite column is a competitive solution for seismic and non-seismic zones, due to the excellent seismic performances (resulted from the presented experimental tests) and also because of improved fire protection. The results obtained on the columns made with high-strength concrete showed improved performances, especially resistance.

A comprehensive study has been conducted to investigate the behavior and strength of a new type of partially encased composite column made with thin-walled, welded I-section, stiffened with transverse links with the link spaced at regular intervals. Concrete is poured between the flanges of the steel section. The paper describes and presents the results of the testing of five large sizes 600×600 mm short column specimens. The parameters considered in the study were the spacing of links and the thickness of flanges. Failure of all specimens was due to local buckling of the flange plates along with concrete crushing. Transverse stresses measured in the steel section were found to be small and did not impair the axial compressive strength of the steel section. High stresses, however, developed in the transverse links as a result of the lateral expansion of the concrete. The study also shows that closer link spacing and the use of additional reinforcements can improve the post-ultimate load behavior (Chicoine, et al., 2002).

Long-Term Behavior and Strength of Partially Encased Composite Columns Made with Built-Up Steel Shapes Investigated by (Chicoine, et al., 2003). A comprehensive study has been conducted to investigate the long-term behavior and strength of partially encased composite columns made with thin-walled welded I sections stiffened with transverse links. The paper presents the strain measurement history and load-deformation response of five 3003*300 mm and two 450*450 mm stub-column specimens. Four specimens were loaded for 150 days, following a typical construction sequence, and five columns were tested up to failure. Long-term axial deformations due to shrinkage and creep of the concrete were recorded and compared to prediction models. The tests showed that the relatively higher stresses in the steel shape due to the sequence of loading and shrinkage and creep of the concrete had no significant effect on the failure mode and ultimate capacity for this type of column. The transverse stresses in the web of the steel shape were lower in specimens subjected to long-term loading. The axial stresses in the transverse links

at peak load, caused by the transverse expansion of the concrete, were found not depend on the loading sequence

The experimental investigation on partially encased composite (PEC) members with thin steel plates and three types of constructional detailing was studied by (Chen, et al., 2010). Six pieces of PEC column specimens were tested under constant vertical load and cyclic horizontal loads. It is found that though local buckling of a thin plate of H steel is a crucial factor when the compressively axial load does not surpass the encased steel capacity, the PEC could behave quite well under cyclic horizontal loads. No distinguished difference in three kinds of details was observed so that PEC members could be built easily. The experimental study reveals that ductile failure mode and comparatively favorable energy dissipation ability can be expected if the width-thickness ratio does not exceed the limitation by Euro code 4, and the axial compression load does not surpass the encased capacity. By analysis followed, it is understood the transverse links play a more important role in the resistance and ductility of PEC members than longitudinal reinforcement and stirrups, so simple construction detail is possible as shown in figure 2.1. The results of the pseudo-static loading tests give a positive reference for evaluating the seismic behavior of the PEC column.

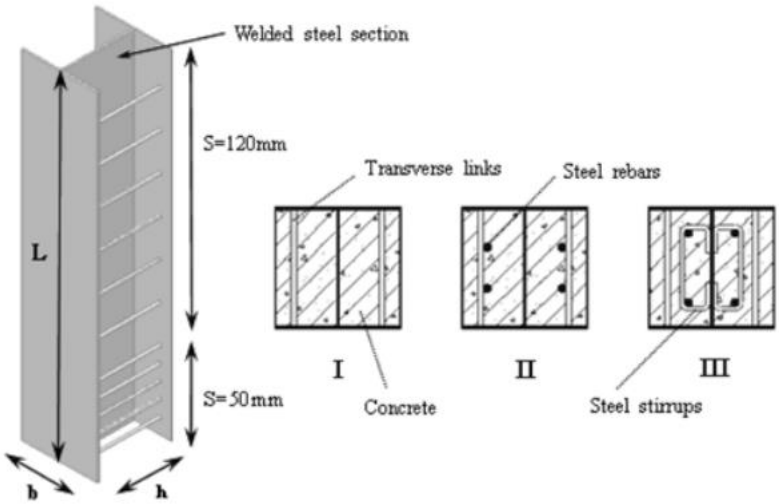

Figure 2. 1 Cross-section of specimens and construction detail (Chen, et al., 2010)

(Y. M. Hunaiti BSc, et al., 1994) Investigated the load-carrying capacity of partially encased composite columns subjected to minor axis bending. IPE 200×100×22 steel sections with a buckling length of 2.4 m were encased partially in concrete and tested to failure under eccentric axial load. The variables studied include the eccentricity of the applied load, eccentricity ratio at the column ends, and the effect of concrete strength. In all tests, tension cracks were observed at loads beyond 70% of the failure load. The maximum strength of the columns was obtained by deflection methods using Newmark's technique of numerical integration.

Structural behavior of partially encased composite columns under axial loads was conducted by (Pereira, et al., 2015). The main objective of the study was to evaluate the influence of replacing the conventional longitudinal and transverse steel bars with welded wire mesh on the structural behavior of these members under concentric loads. To achieve these goals experimental tests on four specimens of partially encased composite columns subjected to axial loading were performed and the results were promising in terms of replacing the traditional reinforcement with steel meshes. The parametrical study results found no significant changes in the behavior of the partially encased columns due to variations of the steel profile thickness or yield strength. However, significant changes in the post-peak behavior were observed when using high-strength concrete and these results suggest a change in the failure mode. It was concluded that the failure mode of partially encased composite columns with thinner plates consists mostly of concrete crushing combined with local buckling of the steel plates. However, the use of transversal links between the flanges, high-strength concrete, or longitudinal and transverse reinforcing bars may change the behavior and load capacity of the composite columns.

Experimental behavior of octagonal partially encased composite columns under axial and bending load conditions was conducted by (Jamkhaneh, et al., 2019). The complementary study on axial and combined axial–torsional behavior is done through finite element analysis. The main parameters for the experiment part are reinforcement details and failure modes. The six parameters of this analytical analysis include the width-to-thickness ratio of a flange, transverse links spacing and diameter, welding line arrangements, and different types of retrofit of cross-shaped steel (concrete encasement, use of stiffener plates, and transverse links). To verify the accuracy of the proposed three-dimensional finite element model, the axial behavior of the numerical models was compared with test specimens. Experimental results of the axial study

show that concrete crushing phenomena and local buckling behavior occurred for all specimens under the ultimate stage of loading. It should be noted that local buckling behavior occurred after the crushing phenomena.

The analysis of bending assessment demonstrated that the use of stirrups has no remarkable effect on increasing the effective bending moment strength of octagonal partially encased composite columns. Meanwhile, an equation was developed based on a comprehensive parametric study of an octagonal partially encased composite column using detailed finite element analyses.

2.2 Numerical Investigation

2.2.1 An overview of ABAQUS

ABAQUS is one of the well-known leading structural analysis systems. The ABAQUS system uses finite element analysis techniques to provide accurate solutions for all types of linear and nonlinear stress, dynamic, and thermal problems. It is an associative feature-based modeler. The model geometry is entered in terms of features that are sub-divided (discretized) into finite elements to perform the analysis. Increasing the discretization of the features will usually increase the accuracy of the solution, but with a corresponding increase in solution time and disk space required. Compared with structural testing, Finite element methods are available to carry out huge experiments without any worry about time and money. Many researchers (Han, 2015), (Ma, et al., 2018), and (Portolés, et al., 2013) all over the world have done much research toward the development of numerical models to simulate the performance of composite columns. By ABAQUS Standard solver, (Zhang, et al., 2011) investigated the axial compressive behavior of short concrete-filled elliptical steel columns, such as the ultimate load capacity, load versus end shortening relationship, and failure modes. Meanwhile, the simulation results are consistent with experimental results, so they stated the simulation results could be used to predict compressive characteristics of short concrete-filled elliptical steel columns.

Analytical methods were developed parallel to the experimental study to determine the strength and behavior of encased composite columns. Successively, a computer analysis method was developed to determine the nonlinear behavior of encased composite columns under different loading conditions. Numerical analyses for PEC columns using the PEC model started very recently as compared to other methods. It has several advantages over experimental research.

However, it was found that very limited research on numerical simulation of PEC column has been conducted.

Numerical investigations on the short PEC column were done by (Maranda 1999), (Chicoine, et al., 2002), and (Begum, et al., 2007). All these researchers conducted finite element analysis to study the behavior of the PEC column.

The first reported numerical study on PEC columns with built-up steel sections was carried out by (Maranda 1999). The finite element model included a quarter of the cross-section between two links in the modeling. The imperfection of the flanges, Residual stresses in the steel section, and contact elements between steel and concrete were addressed. The average numerical peak load obtained from this model was more than the experimental study peak loads. As reported by (Tremblay et al, 1998) some cases the peak load was not reached as the stiffness at the last converged point was observed to be positive.

Numerical study on the behavior and strength of axially loaded concrete encased steel composite columns Conducted by (Rahman, et al., 2017). A nonlinear 3-D finite element (FE) model has been developed to analyze the inelastic behavior of steel, concrete, and longitudinal reinforcement as well as the effect of concrete confinement on fully encased composite (FEC) columns. The model has been verified against the experiments conducted in the laboratory under concentric gravity loads. It has been found that the FE model is capable of predicting the nonlinear behavior of the FEC columns up to failure with good accuracy. The capacities of each constituent of FEC columns such as steel-I section, concrete, and rebar were also determined from the numerical study. Concrete is observed to provide around 57% of the total axial capacity of the column whereas the steel sections contribute to the rest of the capacity as well as to the ductility of the overall system. The nonlinear FE model developed in this study is also used to explore the effects of concrete strength on the behavior of FEC columns under concentric loads. The axial capacity of FEC columns has been found to increase significantly by increasing the strength of concrete. The overall load-carrying capacity of the FEC column is increased by 65% for increasing the concrete strength from 27 MPa to 60 MPa. However, the ductility of the composite column reduces as the strength of concrete increases.

Some numerical studies were carried out on the behavior of the PEC column apart from experimental works. Experimental and numerical studies found that transverse links equally spaced between the flanges and welded along the height of the column provide a very effective way to give lateral support to the free borders of the plates and to reduce the local buckling effects. The thinner plates had the merit of further material saving and structural weight reduction. However thin plates with large width-to-thickness ratios are very sensitive to local buckling of the flanges (Chicoine, et al., 2002), (Begum, et al., 2007). Moreover, the transverse links also provided some confinement to the concrete between the flanges. The effect of parameters such as spacing, size, and shape of the links was also studied. The effects of high-strength concrete on the behavior and load capacity of partially encased composite columns were investigated by (Begum, et al., 2013). In the study, a finite element model including a constitutive model that can predict the overall stress-strain of high strength concrete, the post-peak softening branch, and the residual strength of steel was developed and validated by comparison with experimental results. The parametric study investigated the influence of the high-strength concrete in combination with other parameters such as length-column depth ratio, eccentricity-to-column depth ratio, flange slenderness ratio, and transversal link spacing-to-column depth ratio. Numerical results concluded that the influence of the tested parameters is greatly increased by the use of high strength instead of normal strength (Begum, et al., 2013).

(Song, et al., 2016) investigated Local and post-local buckling behavior of welded steel shapes in partially encased composite columns made with thin-walled, welded H-shapes and concrete encasement between flanges; transverse links are welded between flange tips to reinforce the section. Nonlinear finite element analysis (FEA) was conducted to predict buckling behaviors and strengths of steel shapes. Finite element models were verified through a comparison of FEA results with experimental results. A parametric study was then performed using validated FEA models to investigate the effect of several parameters on the buckling behavior of PEC columns. The residual stress of steel shapes, which is introduced through the welding process, was discussed in detail. The buckling modes of flanges vary a lot due to different link spacing since the half-wavelength of buckled shape is determined by the distance between two links, as illustrated in Fig. 2.2. For flanges without transverse links (see Fig. 2.1(e)), the half-wavelength is extended to about four times the flange width b. As mentioned above, the buckled flange can

continue to carry load due to the stress redistribution in the section. The post-buckling mechanism of the flange is illustrated in fig. 2.3. The section of a flange could be divided into two zones after the initial buckling takes place: a buckled zone in which large deflection developed, and an unbuckled zone at a flange-web junction in which the flange is strongly constrained by the web. 490 specimens with various parameters were analyzed in the parametric study, showing higher critical stress due to smaller width-to-thickness ratio and link spacing, as well as lower yield stress. The effect of welding residual stress, either of mechanical cut plates or flame-cut plates, was comprehensively studied in this work, indicating an adverse effect of residual stress on buckling strength, while the flame-cut type of residual stress was comparatively less effective. Inward and outward imperfections have opposite effects on critical stress.

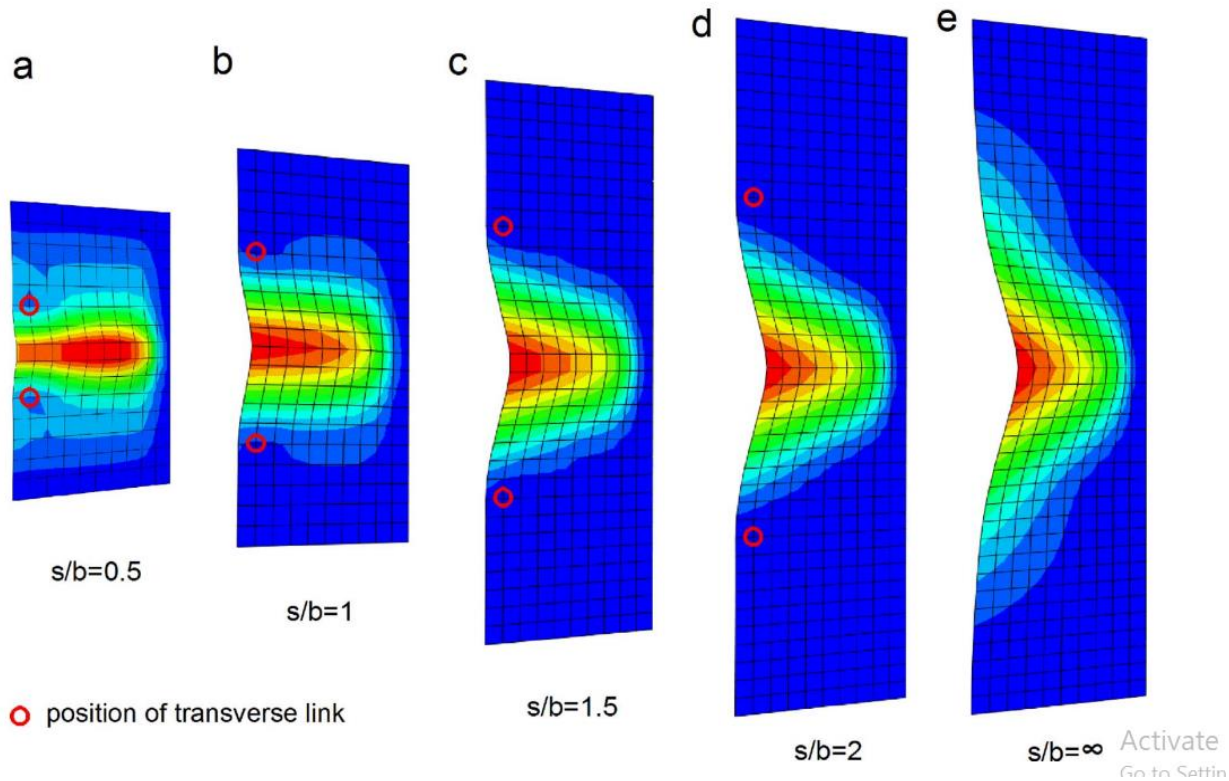

Figure 2.2 Buckling modes of flanges with different link spacing (red color implies relatively large displacement) (Song, et al., 2016)

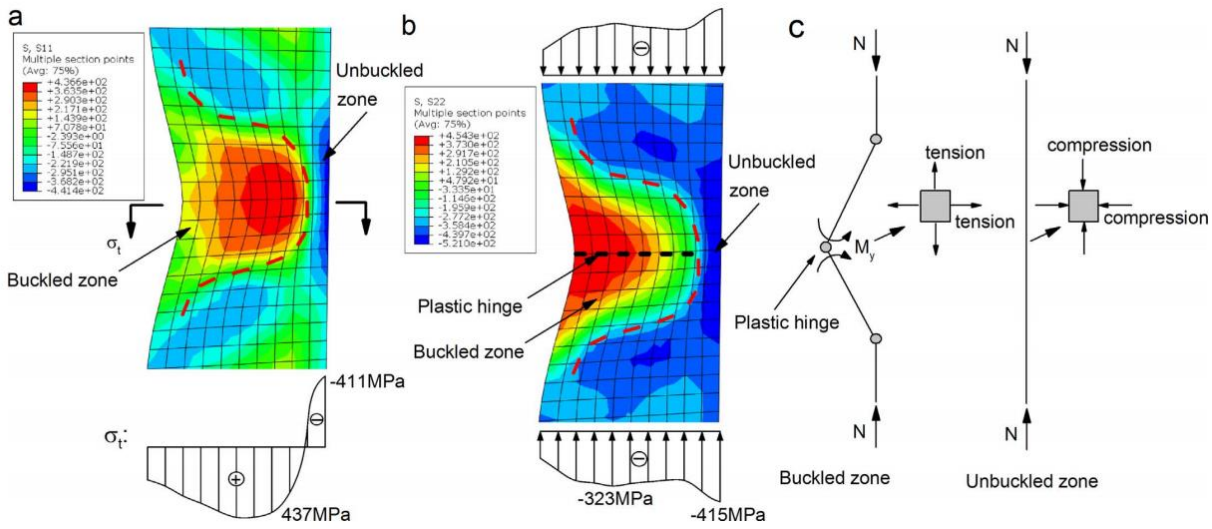

Figure 2.3 Mechanism of post-buckling strength: (a) transverse membrane stress distribution; (b) longitudinal stress distribution; (c) simplified yield mechanism of different zones

Theoretical and analytical studies were undertaken to investigate the structural performance of the concrete-encased composite columns. The main parameters considered in the study were concrete compressive strength and the members with an encased steel section. Finite element software is used to analyze the concrete-encased steel section. Beams and columns were modeled in ANSYS workbench. It is shown that Due to higher load carrying capacity and stiffness, the concrete-encased steel composite members can be suitable for extreme loading conditions (K, et al., 2019).

In addition to experimental investigation, (Pereira, et al., 2015) was developed a numerical FE model using the software DIANA® with FX+. The experimental results were used to validate the numerical model. A satisfactory agreement between experimental and numerical results was observed in both capacity and deformability of the composite columns. Despite the simplifying assumptions of a perfect bond between steel and concrete, the numerical model adequately represented the behavior of the column. A finite element parametric study was performed. Parameters including the thickness of the steel profile, concrete and steel strengths were evaluated.

Summary of experimental and numerical study

- The failure mode of a PEC was due to local buckling of the flange plates along with concrete crushing.
- Most of the studies on the PEC column focus on the parameter width to thickness ratio of steel flange.
- Most of the numerical study was done by nonlinear finite element method software ABAQUS.
- Standard codes to predict the load capacity of partially encased sections limit the width thickness ratio of the plates of steel profile to avoid the occurrence of local buckling. However, the use of thinner plates may reduce the consumption of steel, hence, the overall cost of the column.
- The failure mode of partially encased composite columns with thinner plates consists mostly of concrete crushing combined with local buckling of the steel plates. However, the use of transversal links between the flanges, high-strength concrete, or longitudinal and transverse reinforcing bars may change the behavior and load capacity of the composite columns
- All experimental and numerical research on the PEC column focuses on the behavior and strength of the PEC column by providing horizontal transverse links between the flanges. However, no study focused on the other types of link arrangements.
- In all previous works, researchers used PEC column fabricated with hot rolled shaped cross-section with the same thickness of flange and web. However there is no extensive study focus on the effects of using different thickness of flange and web on the behavior of PEC column.
- In this study different thickness of flange and web used for H-section steel profile.

CHAPTER THREE

RESEARCH METHODOLOGY

3.1 Research Design

The research design is theoretical research that is based on an inductive sampling selection process in terms of which are relevant factors, which are essential for the study of the behavior of a PEC column with different study parameters under axial loading.. This research is a systematic investigation to fill the gap of knowledge on the performance of the PEC column. On the other hand it is a process for collecting, analyzing and, interpreting information to provide a recommendation to the research findings. After comprehensively organizing a literature review of different previous published researches, designate the comparative study of PEC columns with different parameters. Validation for the finite element modeling is conducted on pre-qualified and practical tests for encased composite columns under axial loading. After that specific study parameters introduced for PEC column to investigate the influence of this parameter on the response of PEC columns in cooperative technique.

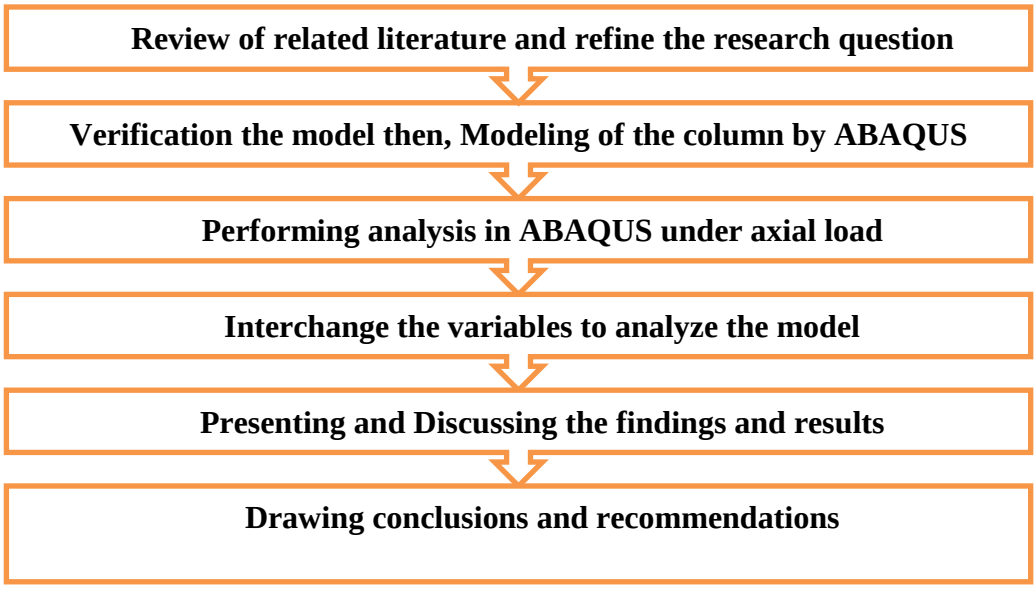

Figure 3. 1 Study design flow chart

3.2. Study variables

3.2.1 Independent variables

The independent variables, which will be measured and manipulated to determine their relationship to observed phenomena, are listed below.

- The thicknesses of the flange (*b/T*) ratio
- The thickness of web (*b/t*) ratio
- Transverse link arrangement

3.2.2 Dependent variables

The dependent variables, which will be observed and measured to determine the effect of the independent variables, are listed below

- Axial load capacity of the PEC column
- Axial load versus axial displacement response
- Failure mode

3.3 Population and Data Collection Process

The finite element method is a numerical analysis technique for obtaining approximate solutions to a wide variety of engineering problems. For this study, a total 14 columns were selected as a sample with the different independent variables. From 14 specimens, one (1) column is from an experimental study for the validation of the model.

Axial loads were applied concentrically on top of the columns. The failure modes, peak load, load-deflection behavior of the specimens were examined in this study. The data collection process for this research was from the secondary sources such as the related topic literature from high-rated journals, ongoing researches, and books.

3.3.1 Model Sample and cross-section used in this study program

The study program consisted PEC columns with five different parameters. The columns were numerically analyzed under axial compressive load. Depending on the parametric study of the model, the whole columns are categorized into three groups. Group one was for investigation of the effect of thickness of flange (*b/T*), group two was for investigation of the effects thickness of web (*b/t*), and group three was for investigation of the effects of stiffener shapes. All columns under the study were modeled with identical material strength. In group three there is no

longitudinal and tie reinforcement while transverse link provided between steel flanges. The cross-section used under this investigation was shown in Figures 3.2 and 3.3 below.

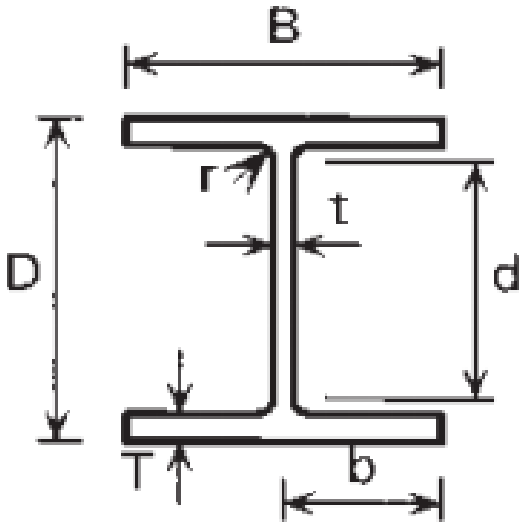

Figure 3.2 H-section (Steel Designers' Manual - 6th Edition, 2003)

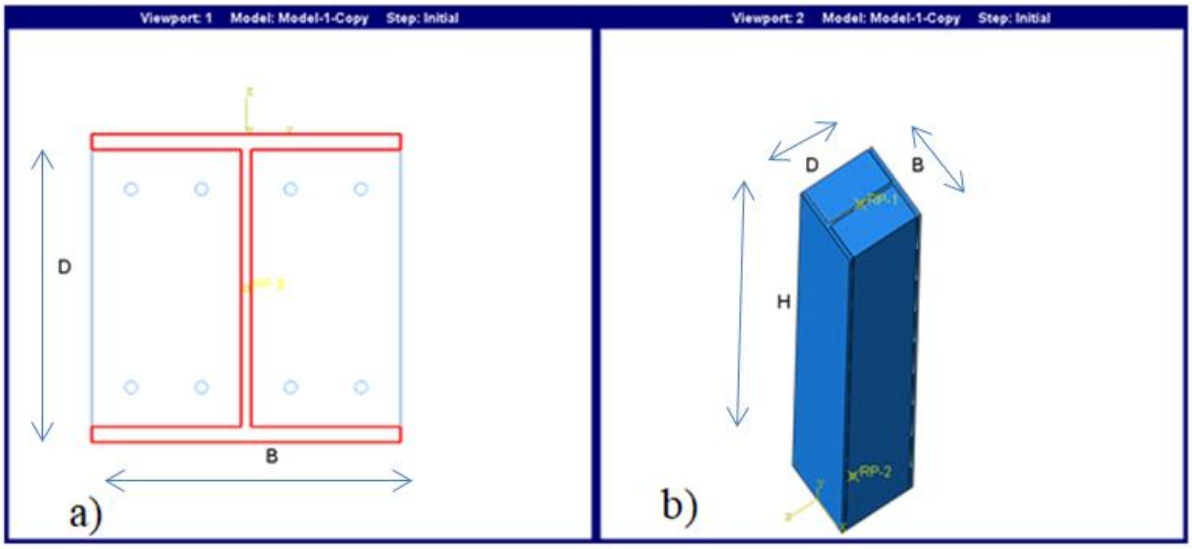

Figure 3.3 a) Cross-section of PEC b) elevation of PEC

Table 3.1 Geometric properties of specimens for investigation of effects of thickness

(Steel Designers' Manual - 6th Edition, 2003)

Serial number	Specimen	Dimension		L (mm)	Thickness (mm)		b(mm)	*b/t*	*b/T*	Rebar Ø (mm)	Stirrup Ø (mm)	Stirrup Spacing S(mm)
		B (mm)	D (mm)		Web (t)	Flange(T)						
GROUP ONE	C-1	209.1	222.2	3000	7.2	11	104.55	14.5	9.5	12	8	101
	C-2	209.1	222.2	3000	7.2	12.5	104.55	14.5	8.4	12	8	101
	C-3	209.1	222.2	3000	7.2	14.2	104.55	14.5	7.4	12	8	101
	C-4	209.1	222.2	3000	7.2	17.3	104.55	14.5	6.0	12	8	101
	C-5	209.1	222.2	3000	7.2	20.5	104.55	14.5	5.1	12	8	101
GROUP TWO	C-6	209.1	222.2	3000	7.2	11	104.55	14.5	9.5	12	8	101
	C-7	209.1	222.2	3000	7.9	11	104.55	13.2	9.5	12	8	101
	C-8	209.1	222.2	3000	9.4	11	104.55	11.1	9.5	12	8	101
	C-9	209.1	222.2	3000	10	11	104.55	10.5	9.5	12	8	101
	C-10	209.1	222.2	3000	12.7	11	104.55	8.2	9.5	12	8	101

Table 3.2 Geometric properties of specimens for investigation of effects of transverse links

	specimen	Dimension		L(mm)	Thickness (mm)		Link spacing, S(mm)	Link diameter Ø(mm)	link arrangement (shape)
		B (mm)	D (mm)		Web (t)	Flange (T)			
GROUP THREE	C-11	209.1	222.2	3000	7.2	17.3	222	12	H
	C-12	209.1	222.2	3000	7.2	17.3	222	12	X
	C-13	209.1	222.2	3000	7.2	17.3	222	12	Z

3.4 Data Processing and Analysis

3.4.1 Finite element method

Finite element analysis is a powerful computer method of analysis that can be used to obtain solutions to a wide range of structural problems involving the use of ordinary or partial differential equations. FE solvers can either use linear or non-linear analysis. Initially, the use of FE required the designer to define the location of every node for each element by hand and, then the data were entered as code that could be understood by a computer program written to solve the stiffness matrix. Nowadays this is often known as the 'solver'. The output was produced as text data only. The use of FEA has been the preferred method to study the behavior of partially encased composite columns (for economic reasons). The Finite Element Analysis (FEA) of partially encased composite column specimens was performed in a nonlinear static analysis format. The analysis procedure considers both material and geometric nonlinearities. In a nonlinear analysis, the total specified loads acting on a finite element body were divided into several load increments. At the end of each increment, the structure is in approximate equilibrium and the stiffness matrix of the structure was modified to reflect nonlinear changes in the structure's stiffness.

The general-purpose finite element program used in this study is to investigate the effect of using different steel thicknesses and different stiffener arrangements on PEC columns under axial loading. Every complete finite-element analysis consists of three separate stages:

Pre-processing or modeling: This stage involves creating an input file, which contains an engineer's design for a finite-element analyzer. Pre-processing involves creating a geometric representation of the structure, assigning properties, and then output the information as formatted data file (.dat).

Processing or finite element analysis (solver): This is a set of linear or nonlinear algebra equations that are solved simultaneously to obtain nodal results, such as displacement values at different nodes or temperature values at different nodes in heat transfer problems.

Post-processing or generating: In this process, the results can be processed to show the contour of displacements, stresses, strains, reactions and, other important information like Graphs, as

well as the deformed shapes of a model can be plotted. A report, images, and animation can be prepared from this output.

3.5 Finite Element modeling of a partially encased composite column

This section describes the finite element model that has developed in the study. It begins with an overview of the process that led to the development of the model followed by a more detailed look at individual aspects of the model; examining first the simplification of the geometry of the physical specimen, followed by a description of the mesh elements used to discretize the geometry, an overview of boundary conditions imposed on the mesh, and a description of the various material models that define the behavior of the model. A complete 3D finite element model was developed in this. Descriptions of the mesh and elements used in the finite element models of the specimens along with the boundary conditions including steel-concrete interaction is presented in the subsequent sections.

A total of 4 parts was used to represent H-section partially encased composite column in the finite element model. The FEM of the partially concrete-encased steel composite columns was carried out by modeling the steel H-section, concrete longitudinal reinforcement bars, stirrups, and, transverse links.

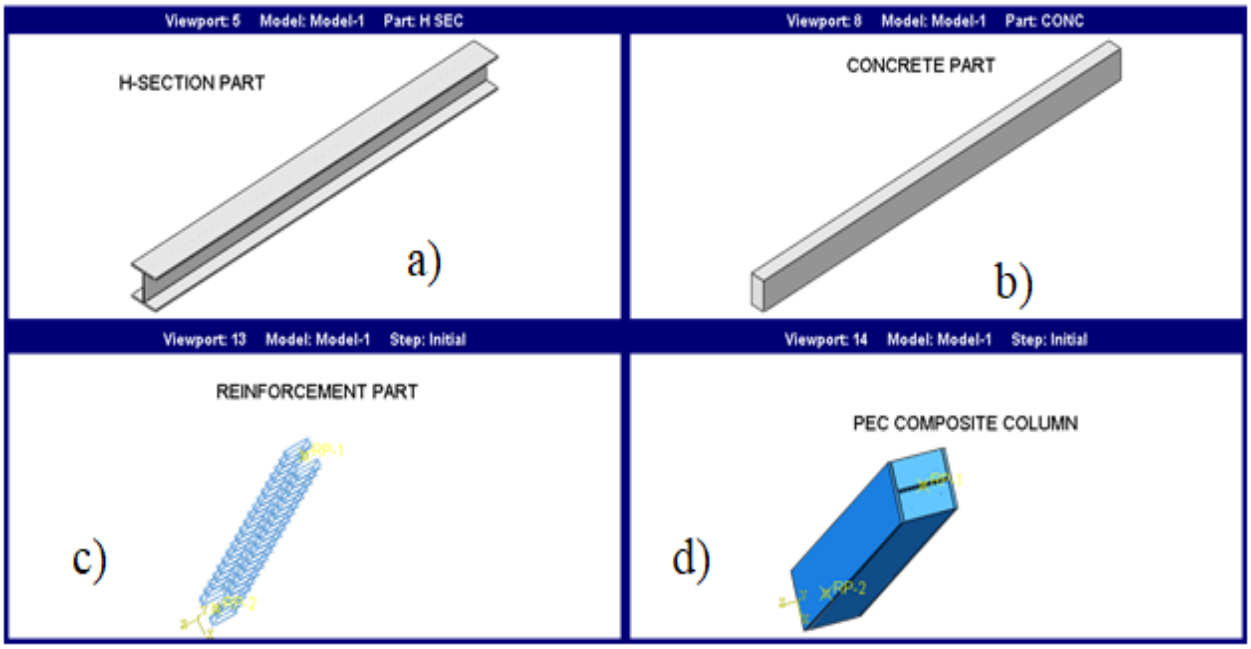

Figure 3.4 parts used in the modeling

3.5.1 Element type and selection

The key in finite element analysis is the appropriate selection of element type. The ABAQUS standard modules consist of a comprehensive element library that provides different types of elements depending to different situations. For reference, it is usual to use a 'beam' element; this will provide results for flexure, shear, and displacement directly. Beam and truss elements are generally triangular or quadrilateral with a node at each corner. However, elements have been developed that include an additional node on each side, this gives triangle elements with six nodes and quadrilateral elements with eight nodes. Since the only places where the forces are accurately calculated are at the nodes (they are interpolated at other positions), the accuracy of the model is directly related to the number of nodes.

By introducing more nodes into an element, the accuracy of the results is increased. Alternatively, to reduce computational time the number of element should be reduced. For this reason, 3D 8-noded hexahedral (brick)elements having 3 degrees of freedom in each node (translations in X, Y, and Z directions) are utilized for modeling concrete elements and steel sections with reduced integration (C3D8R) to prevent the shear locking effect.

To model reinforcements and transverse links, 2-noded truss elements (T3D2) having 3 degrees of freedom in each node (translations in X, Y, and Z directions of global coordinates system) was used. The embedded method with a perfect bond between reinforcement and surrounding concrete is adopted to properly simulate the reinforcement-concrete bonding interaction. ABAQUS has an extensive library of elements that can be used to model concrete, including both continuum and structural elements. Elements are classified first by the "family" to which they belong.

3.5.2 Material Modeling

The material definition is an important part of finite element analysis, and each component should be defined carefully and all parts should be defined with appropriate material parameters. Steel, concrete and rebar are the main materials used in the PEC columns for this study. The nonlinear behavior of these three materials can be incorporated in the FE model using the appropriate material models for steel, concrete, and rebar that available in the ABAQUS (HKS 2013) finite element code. The description of the material models for steel and concrete along

with their mechanical properties (stress versus strain relationship) used in the FE model is described in the following sections.

3.5.3 Compression properties of concrete

Concrete is one of our most common building materials and is used both for buildings, bridges, and other heavy structures. Typically, concrete structures are very durable, but sometimes they need to be strengthened. Concrete is a material that can withstand compressive loads very well but is sensitive to tensile forces. Therefore, concrete structures are typically reinforced by casting in steel bars in areas where tension can arise. Concrete experiences different characteristics in confined and unconfined conditions. But for this study, since the concrete in the composite section is very small it is modeled as confined concrete as a whole in the column.

3.5.4 Unconfined properties of concrete in the concrete cover section

(ES EN1992, 2015) used in this study for the unconfined concrete, the relation between δ_c and ε_c under uniaxial loading as described in (ES EN1992, 2015), and it proposed a single equation to describe unconfined concrete stress-strain behavior as follows by expression (3.1). Based on uniaxial compression test results one can accurately determine how the material behaved. However, a problem arises when the person running such a numerical simulation has no such test results or when the analysis is performed for a new structure. Then often the only available quantity is the average compressive strength (f_{cm}) of the concrete. Another quantity that must be known to begin an analysis of the stress-strain curve is the modulus of elasticity (*Ecm*) of the concrete. Its value can be calculated using the relations available in the literature (ES EN1992, 2015).

$$\frac{\delta c}{f_{cm}} = \frac{k\eta - \eta^2}{1+(k-2)\eta} \tag{3.1}$$

$$\eta = \frac{\varepsilon_c}{\varepsilon_{c1}} \tag{3.2}$$

$$k = 1.05E_{cm} * \frac{|\varepsilon_{c1}|}{f_{cm}} \tag{3.3}$$

$$E_{cm} = 22(0.1f_{cm})^{0.3} \tag{3.4}$$

$$\varepsilon_{c1} = 0.7(f_{cm})^{0.31} \tag{3.5}$$

$$f_{cm} = f_{ck} + 8 \quad (3.6)$$

Where,

ε_{c1} is the strain at the average compressive strength

f_{cm} is the mean value of concrete cylindrical comparative strength (Mpa)

E_{cm} is the longitudinal modulus of elasticity (Mpa)

f_{ck} is characteristic cylindrical strength of concrete(Mpa). All of the equation was from (ES EN 1992-1-1:2015). The above equation is valid for $0 < \varepsilon_c < \varepsilon_{cu}$ where ε_{cu} is the nominal ultimate Strain and$\varepsilon_{cu} = 3.5\%$. Figure 3.5 describes the developed stress-strain relationship as provided in (ES EN1992, 2015). The specific development of stress-strain relationship for this study was provided in appendix A.

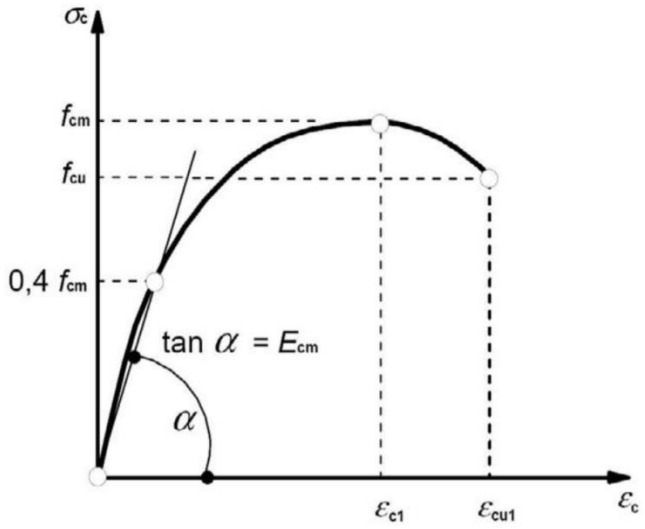

Figure 3.5 Stress-strain relation for non-linear structural analysis (ES EN1992, 2015)

3.5.5 Confined properties of concrete in column

The confinement of the concrete by stirrups has been recognized in early research. This confinement can provide a confining pressure which leads to an enhancement in the strength and ductility of concrete (Chen, et al., 1999). Confinement of concrete results in a modification of the effective stress relationship: higher strength and higher critical strains are achieved. The other basic material characteristics may be considered as unaffected for design. For PEC columns, the amount of the confining pressure depends on the steel section shape and its yield strength in addition to the factors mentioned earlier. As a result, a highly confined zone occurs resulting

from arching action formed by the steel section. In the absence of more precise data, the stress-strain relation shown in Fig. 3.5 (compressive strain shown positive) may be used, with increased characteristic strength and strains according to:

$f_{ck}, c = f_{ck}(1.00 + 5\delta_2/f_{ck})$ for $\delta_2 \leq 0.05 f_{ck}$ 3.7

$f_{ck}, c = f_{ck}(1.25 + 25\delta_2/f_{ck})$ For $\delta_2 \geq 0.05 f_{ck}$ 3.8

$\varepsilon_{c2,c} = \varepsilon_{c2}\,(f_{ck}, c/f_{ck})^2$ 3.9

$\varepsilon_{cu2,c} = \varepsilon_{cu2}\,\delta_{2f}/f_{ck}$ 3.10

Where $\boldsymbol{\delta_2 = \delta_3}$ is the effective lateral compressive stress at the ULS due to confinement and $\varepsilon c_{2,}c$ and $\varepsilon cu_{2,}c$ follow from code provision. ε_{c2} =2% and ε_{cu2} =3.5%

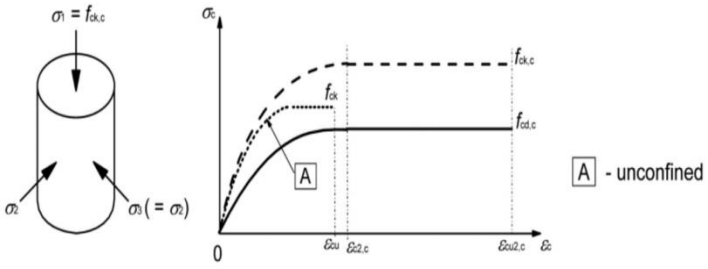

Figure 3.6 Stress-strain relationship for Confined Concrete (ES EN1992, 2015).

3.5.6 Tension properties of concrete

ABAQUS provides several options for defining the tensile behavior of concrete. The stress can be related to the strain in the direction of the cracking or displacement which refers to crack width and fracture energy $\boldsymbol{G_f}$. Alternatively, the fracture energy $\boldsymbol{G_f}$ can be specified directly as a material property; in this case, define the failure stress, as a tabular function of the associated fracture energy. This model assumes a linear loss of strength after cracking (ABAQUS software (SIMULIA, 2014)). The cracking displacement at which complete loss of strength takes place is, therefore $\boldsymbol{\varepsilon_{to} = 2G_f/\delta_{to}}$ typical values of $\boldsymbol{G_f}$ range from 40 N/m to 120 N/m. If tensile damage $\boldsymbol{d_t}$ is specified, Abaqus automatically converts the cracking displacement values to "plastic" displacement values using the relationship:

$$\varepsilon_t^{pl} = \varepsilon_t^{ck} - \frac{d_t}{1-d_t} * \delta_t / E_O \quad 3.11$$

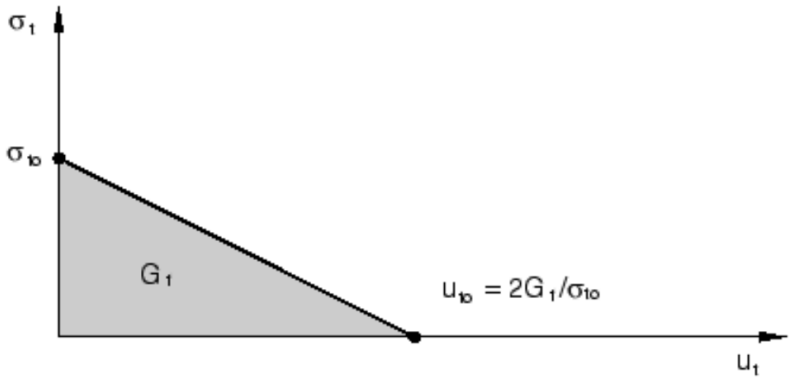

Figure 3.7 Post failure stress-fracture energy curve. (ABAQUS user Manual, 2014)

3.5.7 Tension Stiffening Relationship

To simulate the complete tensile behavior of reinforced concrete in ABAQUS, a post-failure stress-strain relationship for concrete subjected to tension (similar to Figure 3.8) is used which accounts for tension stiffening, strain-softening, and steel concrete interaction with concrete. To develop this model, the user should input young's modulus ($\boldsymbol{E_o}$), stress ($\boldsymbol{\delta_t}$), cracking strain ($\boldsymbol{\varepsilon_t^{ck}}$) values and the damage parameter values ($\boldsymbol{d_t}$)for the relevant grade of concrete. The cracking strain($\boldsymbol{\varepsilon_t^{ck}}$) calculated from the total strain using (equation 3.12) below

$$\varepsilon_t^{ck} = \varepsilon_t - \varepsilon_{ot}^{el} \quad 3.12$$

$$\varepsilon_{ot}^{el} = \delta_t / E_o \quad 3.13$$

ε_t=total strain

Having defined the yield stress-inelastic strain pair of variables, one needs to define now degradation variable dc. It ranges from zero for an undamaged material to one for the total loss of load-bearing capacity (Kmiecik, et al., 211). These values can also be obtained from uniaxial compression tests, by calculating the ratio of the stress for the declining part of the curve to the compressive strength of the concrete. Thanks to the above definition the CDP model allows one to calculate plastic strain from the formula:

$$\varepsilon_t^{pl} = \varepsilon_t^{ck} - \frac{d_c}{(1-d_{c)}} \frac{\delta_t}{E_o} \quad 3.14$$

Where $\boldsymbol{E_o}$ stands for the initial modulus of elasticity for the undamaged material. Knowing the

plastic strain and having determined the flow and failure surface area one can calculate stress $\boldsymbol{\delta_t}$ for uniaxial compression and its effective stress $\overline{\boldsymbol{\delta_t}}$.

$$\delta_t = (1-d_c)\, E_o(\varepsilon_t - \varepsilon_t^{pl}) \qquad 3.15$$

The damage plasticity constitutive model was based on Equation 3.16 stress-strain relationship:

$$\overline{\delta_t} = \frac{\delta_t}{(1-d_c)} = E_o(\varepsilon_t - \varepsilon_t^{pl}) \qquad 3.16$$

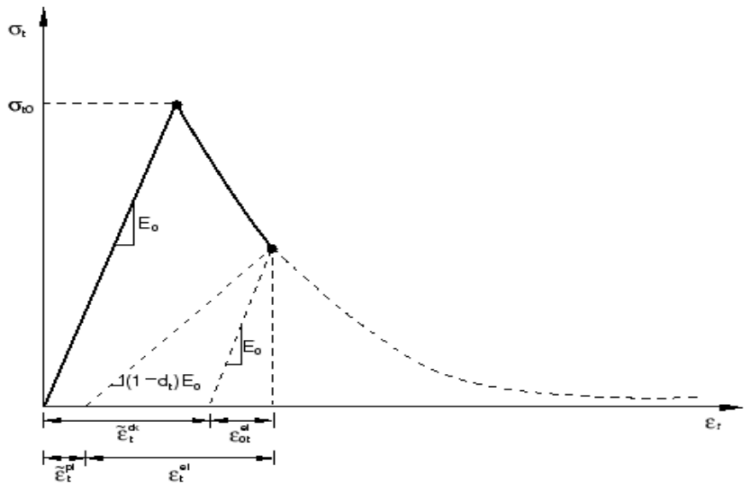

Figure 3.8 Terms for Tension Stiffening Model (ABAQUS user Manual, 2014)

Where $\boldsymbol{dt}$ and $\boldsymbol{dc}$ are two scalar damage variables, ranging from zero (undamaged) to one (fully damaged) (Hafezolghorani, et al., 2017).

The damage model used for concrete was based on plasticity and considered the failure process of tensile cracking and compressive crushing. The uniaxial compressive and tensile responses of concrete concerning the concrete damage plasticity model subjected to compression and tension load were given by:

$$\varepsilon_c^{pl} = \varepsilon_c^{ck} - \frac{d_c}{(1-d_c)}\frac{\delta_c}{E_o} \qquad 3.17$$

$$\delta_c = (1-d_c)\, E_o(\varepsilon_c - \varepsilon_c^{pl}) \qquad 3.18$$

$$\overline{\delta_c} = \frac{\delta_t}{(1-d_c)} = E_o(\varepsilon_c - \varepsilon_c^{pl}) \qquad 3.19$$

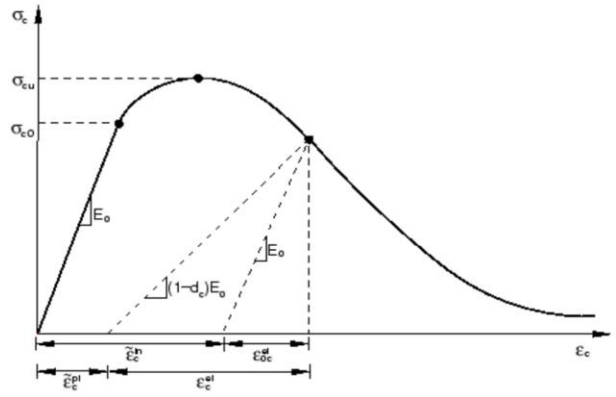

Figure 3.9 Response of concrete to a uniaxial loading condition in compression (ABAQUS user Manual, 2014)

Another parameter describing the state of the material is the point at which the concrete undergoes failure under biaxial compression. (f_{bo} / f_{co}) The ABAQUS user's manual specifies the default value (f_{bo} / f_{co})=1.16. The last parameter characterizing the performance of concrete under compound stress is the dilation angle, i.e. the angle of inclination of the failure surface towards the hydrostatic axis, measured in the failure plane. Physically, the dilation angle (ψ) is interpreted as a concrete internal friction angle. In simulations usually ψ= 36° 0, 0 or ψ= 40° is assumed.

Table 3.3 Default parameters of CDP model under compound stress (Kwaśniewski, et al., 2011)

Dilation angle	Eccentricity	f_{bo}/f_{co}	K	Viscosity parameter
36	0.1	1.16	0.667	0

Table 3.4 Mechanical properties of concrete

Part	characteristic compressive strength (N/mm^2)	Density (kG/m^3)	Young Modulus (GPa)	Poisson's Ratio
concrete	25	24	31	0.2

3.5.8 Structural Steel and Reinforcement material modeling

The structural steel section and the reinforcement bars are modeled as an elastic-plastic material in tension and compression as given in Euro code 3, 2005, ABAQUS Manual, 2014, and Euro code 2, 2005. Steel is a ductile material that experiences large inelastic strain beyond the yield point. So the true stress and logarithmic strain graph which is also called the hardening curve, as shown in Figure 3.9, is considered for modeling the material behavior of steel.

The stress-strain responses in compression and tension are assumed to be the same. This response exhibits a linear elastic portion followed by the strain hardening stage until reaches the ultimate stress. The metal plasticity model in ABAQUS was used to define the non-linear behavior of materials. The "ELASTIC" option was used to assign the given in the table 3.4.

The "PLASTIC" option is also used to define the plastic part of the stress-strain curve. According to the ABAQUS manual ABAQUS, 2014, true stress and true strain should be used to define the non-linear behavior of material properties. So, the true stresses were assigned in ABAQUS as a function of the true plastic strain.

To investigate numerically the post-buckling behavior of the columns it is necessary to represent correctly the inelastic material properties in the FE models. The Mises yield surface is defined by giving the value of the uniaxial yield stress as a function of the uniaxial equivalent plastic strain. The curve in Figure 3.9 named "ABAQUS input" depicts the relation between true stress ($\boldsymbol{\delta_{true}}$) and true plastic strain($\boldsymbol{\varepsilon_{true}}$). The stress and strain data obtained from the uniaxial tension tests are converted to true stress, $\boldsymbol{\delta_{true}}$ and logarithmic plastic strain, $\boldsymbol{\varepsilon_{true}}$, the relationship between the two is given in Equation 3.22 and 3.23.

$$\delta_{true} = \delta_{nom}\,(1+\varepsilon_{nom}) \qquad 3.22$$

$$\varepsilon_{true} = \ln(1+\varepsilon_{nom}) \qquad 3.23$$

Where, δ_{true} Nominal or engineering stress

ε_{true} Nominal or engineering strain

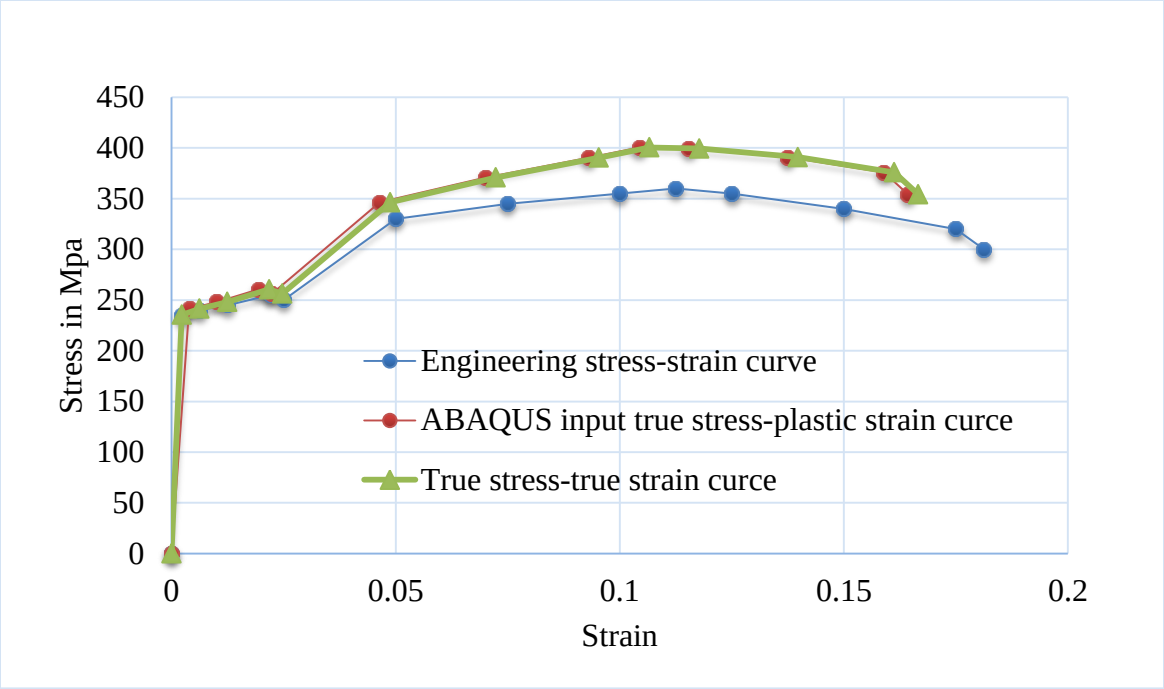

Figure 3.10 ABAQUS input Stress - strain curves for steel structure (Kwaśniewski, et al., 2011)

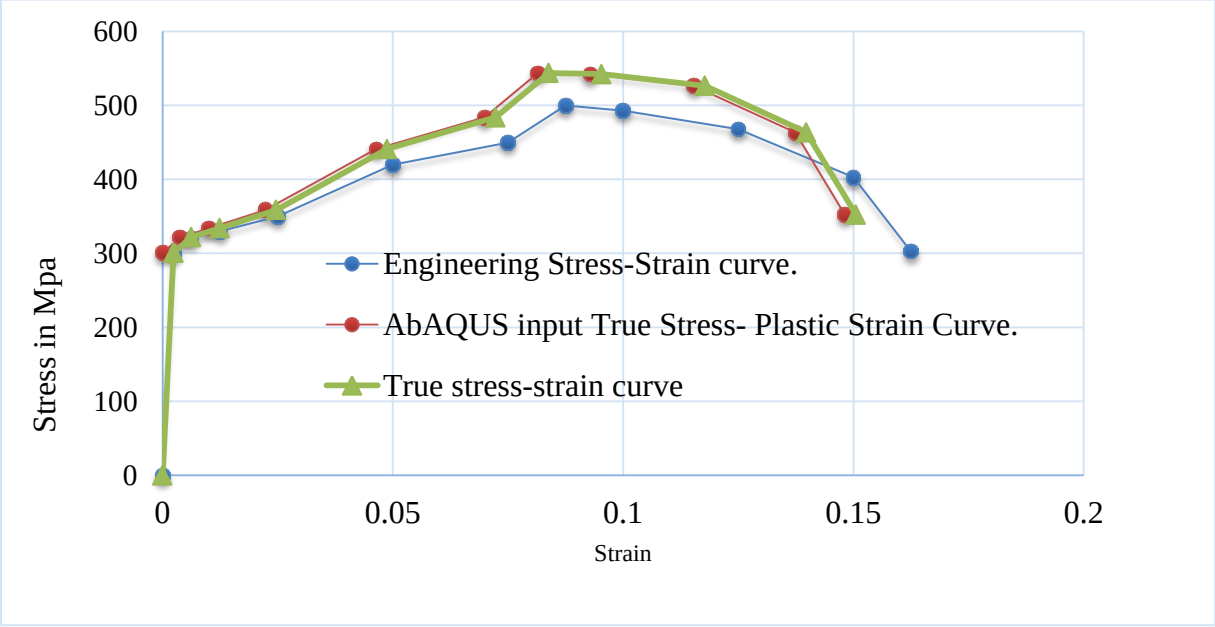

Figure 3.11 ABAQUS input Stress - strain curves for reinforcement (Kwaśniewski, et al., 2011).

Table 3.5 Mechanical properties of steel and reinforcement

Part	Yield Stress (N/mm^2)	Ultimate Stress (N/mm^2)	Density (kG/m^3)	Young Modulus (kN/mm^2)	Poisson's Ratio
Steel Structure	235	360	7850	210	0.3
Reinforcement and Links	300	500	7850	200	0.3

3.5.9 Interactions and Kinematic Constraints between Components.

Kinematic relationships between the various components are required to be defined within the finite element model to ensure strain compatibility between the various components. In other words, interactions had to be defined such that the equal and opposite loading applied between the bodies results in one or more bodies deforming together. The interactions that utilized in the construction of the model were embedded constraints that were used to define the interaction between the concrete and the steel reinforcement. The second one is the surface-to-surface interaction between structural steel and concrete. The third one is tie constraint that used to connect the transverse link with steel structure.

Embedded Constraint

The elements used for rebar and the concrete section of the PEC columns defined using the embedded element option in ABAQUS Standard (ABAQUS user's manual (2014)). This option ensures bonding between the concrete and reinforcement parts of the column.

Transverse link and rebar were defined in infill concrete block as 'embedded' reinforcement which effectively couple the longitudinal behavior of rebar with that of adjacent concrete. The embedded element technique is used to specify an element or groups of elements embedded in host elements. In PEC columns, the concrete defined as the host element whereas the transverse link and reinforcement defined as the embedded elements.

Surface To Surface Contact

The second interaction defined in the model takes the form of a surface-based constraint in which a constraint is formed between two surfaces on the geometry, a master and a slave surface. First, the surfaces of different components that can be in contact must be created and interaction property defined. In this study, the interior part of the steel structure is taken as master surface

and concrete is defined as slave surface with the surface to surface contact ABAQUS standards. After that pairs of surfaces which are going to be in contact must be identified. Two components define the mechanical interaction of contacting surfaces, which are normal to the surfaces and tangential to the surface. In ABAQUS the default normal interaction between the surfaces is called the 'hard contact', meaning that the surfaces can contact each other when the clearance between them becomes zero and they can transmit between each other the unlimited magnitude of pressure but cannot penetrate each other. For interaction, surface-to-surface contact was created between the structural steel profile and concrete with tangential behavior. The penalty method (also known as the stiffness method) is used for imposing frictional constraints. This stiffness method allows the relative motion between the surfaces of two materials even when they are sticking.

Tie constraint

The steel flange and transverse link was connected by tie constraint. To ensure the bond between steel and transverse link node to node constraint used. The flange was considered as master surface while the transverse link considered as slave surface.

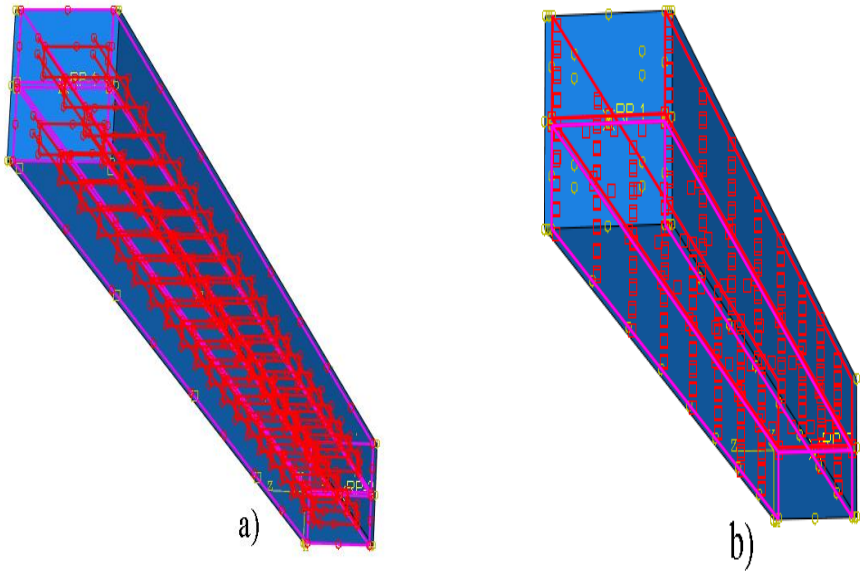

Figure 3.12 Kinematic constraints between components a) surface to surface interaction between steel structure and concrete b) embedded region

3.6 Boundary Conditions and Loading

How the bodies within the finite element model interact with each other and with the imposed boundary conditions can impact both the results and stability of the analysis. The first was reactionary boundary conditions that are constant conditions externally imposed on the model. Another type of external boundary condition is those intended to load the structure and change during analysis.

The boundary condition was applied at rigid body constraint reference point with all degree of freedom fixed and an axial load was exerted through displacement control loading strategy at rigid body reference point at the center of the top end of the column. Uniformity of vertical displacement through the section was ensured and the loading rate could be controlled precisely. The horizontal translations at the top surface were fixed. Since the load is applied at the top the vertical restraint should be released.

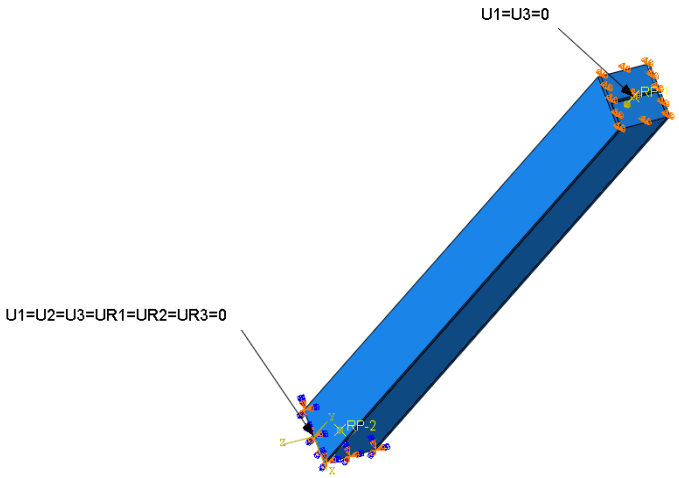

Figure 3.13 Boundary condition and loading

3.7 Meshing

Two bodies needed to be discretized through meshing in this study. These are line bodies and solid bodies. Line bodies can be represented by beam and/or truss elements, solid bodies can mesh with a variety of solid elements ranging from four-node tetrahedral elements to polyhedral shapes. In ABAQUS meshing can be done individually on parts and then assembled or vice-versa. In this analysis, parts were individually meshed and then assembled for further process. Meshes are composed of tri-dimensional continuum solid elements with 8 nodes called C3D8R,

8 nodes linear brick elements with reduced integration were used for both materials, concrete, and steel structure. T3D2, 2-node linear 3-D truss element were used for reinforcement and transverse link. The Engineer has to assess how fine the mesh should be; a coarse mesh may not give an accurate representation of the forces, especially in locations where the stresses change quickly in a short space e.g. at supports, near openings, or under-point loads. This is because there are insufficient nodes and the results are based on interpolations between the nodes. However, a very fine mesh takes excessive time to compute. For this study the mesh size for concrete was 35mm and, for steel structure and reinforcement were 30mm.

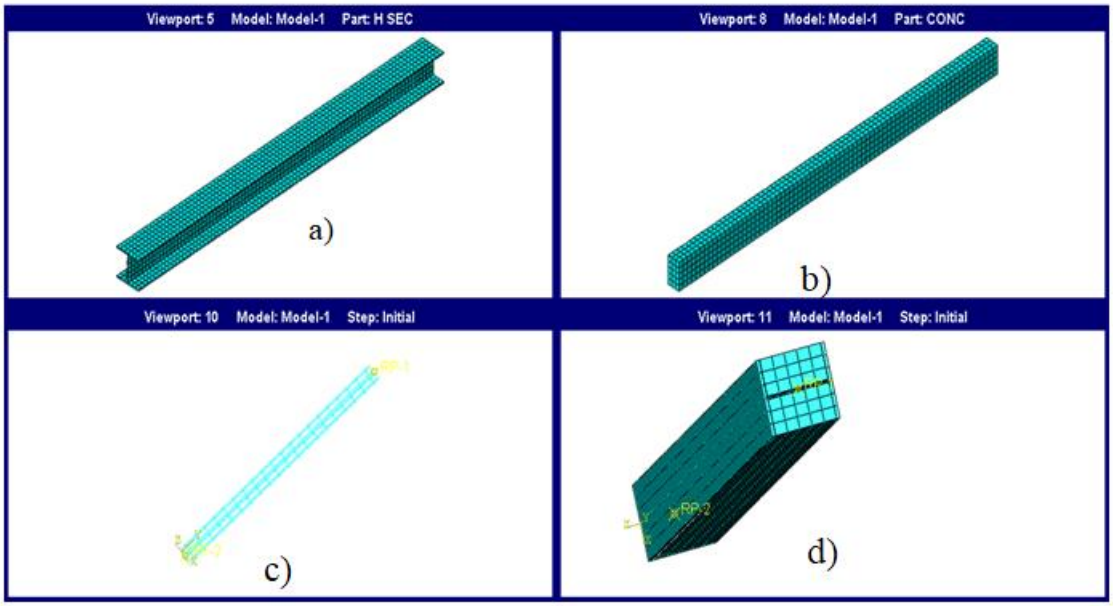

Figure 3.14 Finite element mesh a) steel structure b) concrete c) reinforcement c) PEC column

3.8 Parametric study

The design of the parametric study for this study was the column with section dimension was given in Table 3.1. The height of all the columns was uniform with 3000mm. These columns were designed and analyzed during the parametric study to incorporate the effects of several geometric parameters that affect the PEC column behavior. The geometric variables were the thickness of structural steel, transverse link shapes with horizontal, X-shape, and Z-shape. (Tables 3.1) specimens divided into three groups (Group one and two) were analyzed to observe the effects of width to the thickness of flange (*b/T*) and width to thickness of web (*b/t*) ratio respectively, while groups three designed to investigate the effects of link arrangements on the

response of PEC composite column. Typical cross-section and elevation of the PEC column used in the parametric study are shown in Figures 3.1 and 3.2.

Structural Steel thickness

Steel structure thickness used in this study is defined as the ratio of the width to the thickness of flange (*b/T*) and width to thickness of web (*b/t*). All the columns in this group were constructed by 12mm diameter of longitudinal reinforcement and 8mm diameter of transverse reinforcement with a spacing of 101 mm and 25mm concrete cover was provided. Five different width to thickness ratios of the flange from (5.1mm to 9.5mm) and five widths to a thickness of web from (8.22mm to 14.51mm) were employed in the parametric study (Table 3.1) of group one and two specimens.

Link arrangement

Three types of link arrangements (horizontal, X-shape and, Z-shape) are considered as shown in figure 3.16 with spacing equal with a depth of the cross-section (222mm). X-shape and Z-shape links are inclined with an angle of 45 degrees. To investigate the effects of transverse links group three specimens analyzed with three types of link arrangements which made up of rebar of 12mm diameter rebar. To protect the links from the external environment, 25mm concrete cover was provided.

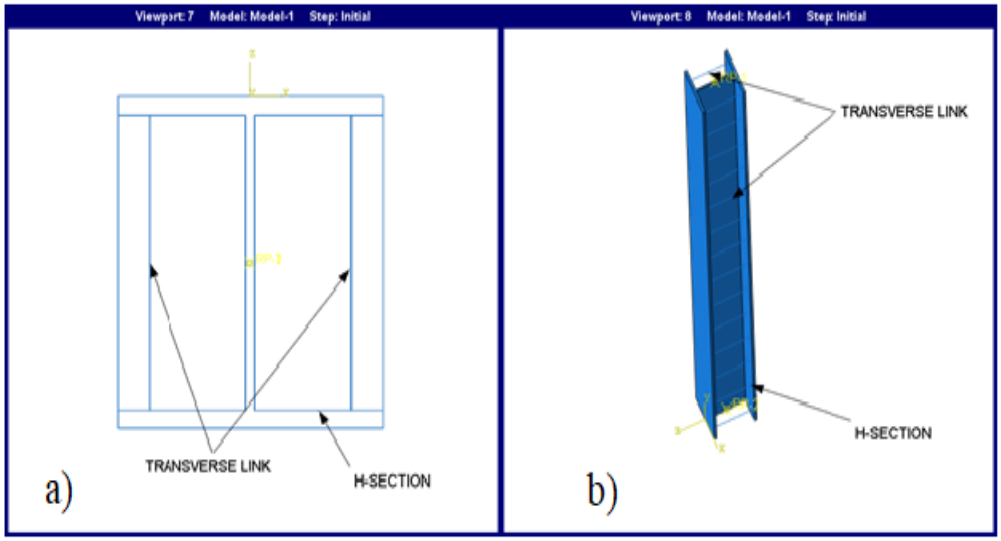

Figure 3.15 cross-sections and elevation of link

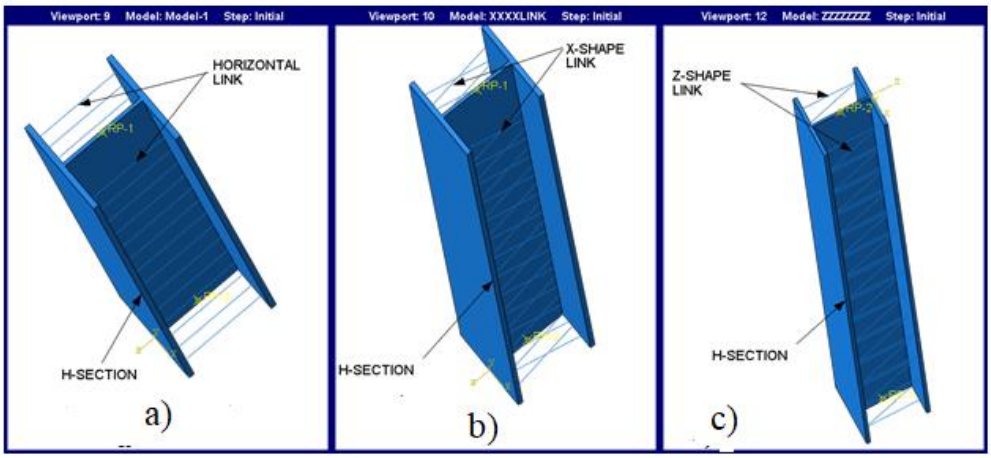

Figure 3.16 Link shapes a) horizontal b) X-shape c) Z-shape

3.9 Model verification

3.9.1 Verification of FEM of the Encased Composite Columns

The aim is to prove that the model developed in this study using the finite element program ABAQUS is valid for the analysis of the fully encased composite columns. The finite element models of encased composite columns developed in this study were verified against tests detailed in (Rahman, et al., 2016). To validate the model and ensure that the model can be considered accurate representation of the system's behavior, the results predicted by the finite element model were compared against the experimental results. The details of the specimen geometry and, material properties of encased composite columns are shown in Tables 3.5 and 3.6.

The comparison of experimental and numerical load-deflection behavior and failure behavior of the FEC column is illustrated in Figures 3.18 through 3.20. It was observed that the FE model can predict the experimental behavior of the composite column with good accuracy. The peak axial capacity and peak axial deformation of these columns matched well with corresponding experimental results. The peak axial load from experimental investigation was 477kN and the peak axial load from FE was 510kN. The difference in percentage between peak load from experimental and FE was 6.47 %. In addition, it is observed from the failure behavior of concrete compressive damage that the failure pattern of concrete from the FE model is matching well with the failure pattern of concrete from the experimental study.

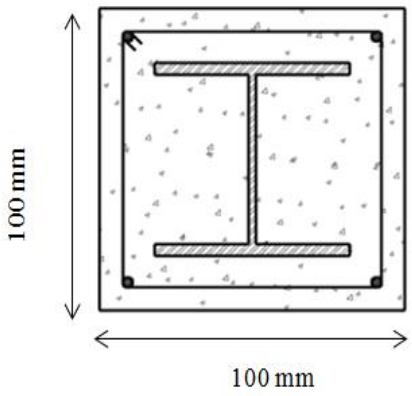

Figure 3.17 Cross-section from test specimen (Rahman, 2016)

Table 3.6 Cross-section of test specimen

Dimension				Reinforcement	
B(mm)	D(mm)	L(mm)	Steel section (mm)	longitudinal	Transverse
100	100	900	20x20x5x5	4-φ8mm	φ6mm@50mm

Table 3.7 Material properties of a test specimen (Rahman, 2016)

Part	Yield Stress N/mm^2	Ultimate Stress N/mm^2	Density Kg/m^3	Young Modulus KN/mm^2	Poisson's Ratio
Steel Structure	350	626	7850	210	0.3
Reinforcement	350	626	7850	200	0.3
Concrete			24	24.68	0.2

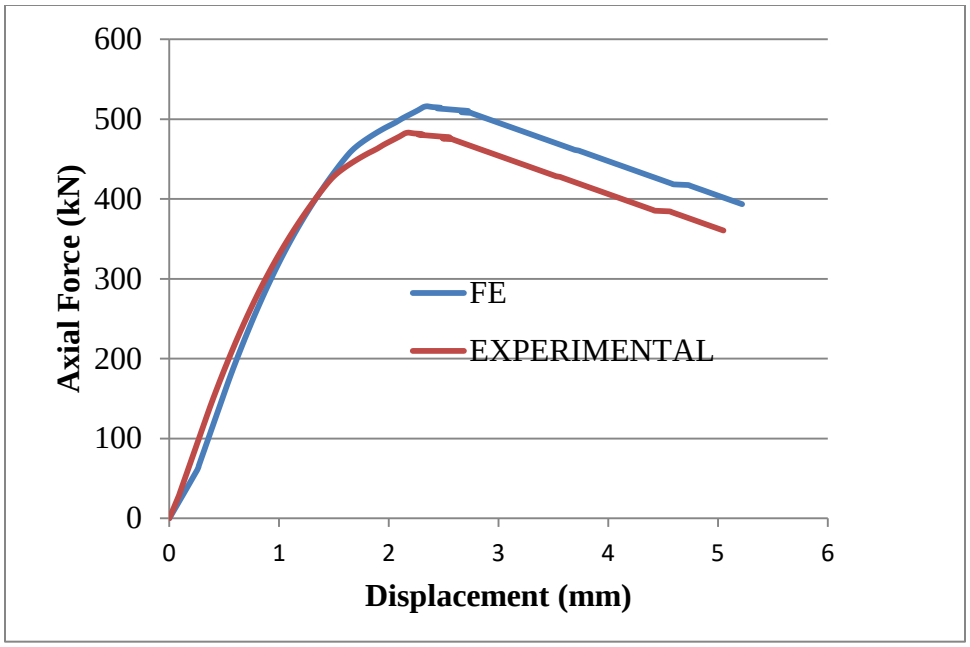

Figure 3.18 Load deformation curve

Figure 3.19 Failure mode of a column from experimental study (Rahman, et al., 2016)

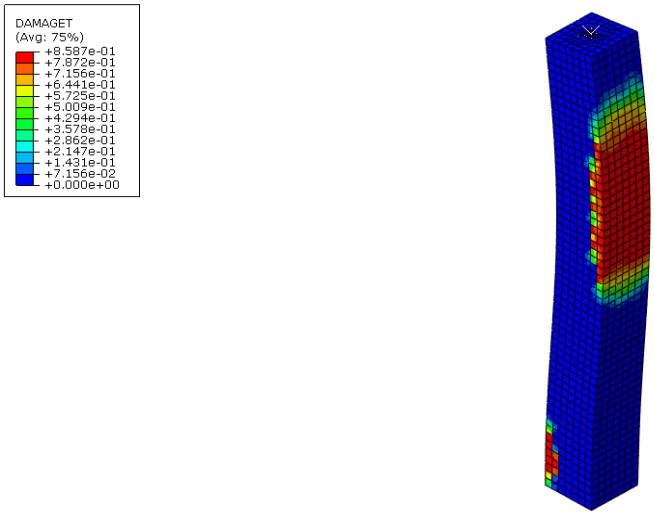

Figure 3.20 Failure mode of column from FE specimen C-14

CHAPTER FOUR

RESULT AND DISCUSSION

The main aim of this study was to investigate the response of the PEC column under axial loading, by considering the effects of the thickness of structural steel and the effects of transverse link shape. In this study, four results have been discussed. From the FE analysis result, axial load versus axial displacement, failure behavior, concrete compressive damage and, concrete tensile damage of PEC column have been presented. Observations are made through the aid of plots of output data, tabular form, and photographs in developing relationships between parameters and behavior.

4.1 Effects of thickness

Group one and two of the specimen in table 3.1 were analyzed to investigate the effects of the thickness of flange and web on the behavior of the PEC column. For this study, five different *b/T* ratios (9.5, 8.4, 7.4, 6.0, and 5.1) and five different *b/t* ratios (14.5, 13.2, 11.1, 10.5, and 8.2) were considered by varying the thickness of flange and web. As observed from non-linear FE analysis, the capacity of the PEC column is controlled by the overall thickness ratio. A detailed discussion has given in the following section.

4.1.1 Load-deformation response

Effect of width to thickness ratio of flange (*b/T*) and width to thickness ratio of the web (*b/t*) in terms of load versus deformation response illustrated in the Figures 4.1 and 4.2 respectively. The value of maximum load and displacement for each specimen are shown in the Figure 4.1 and 4.2. The peak load is the maximum loading attained in the nonlinear analysis of PEC column and the peak displacement is the maximum displacement attained at the maximum loading. When b/t and *b/T* decreases the specimen's maximum compressive load increases. Percentage difference in peak load capacity of group one and two were given in the Table 4.1. With the increase of the *b/T* or *b/t* ratio of the steel, the steel section occupies a small ratio in the entire cross-section and the capacity of the section decreases due to the early failure concrete. This indicates that for the loading capacity the steel ratio plays a crucial role. The ductility of the column increased as thickness ratio decreased.

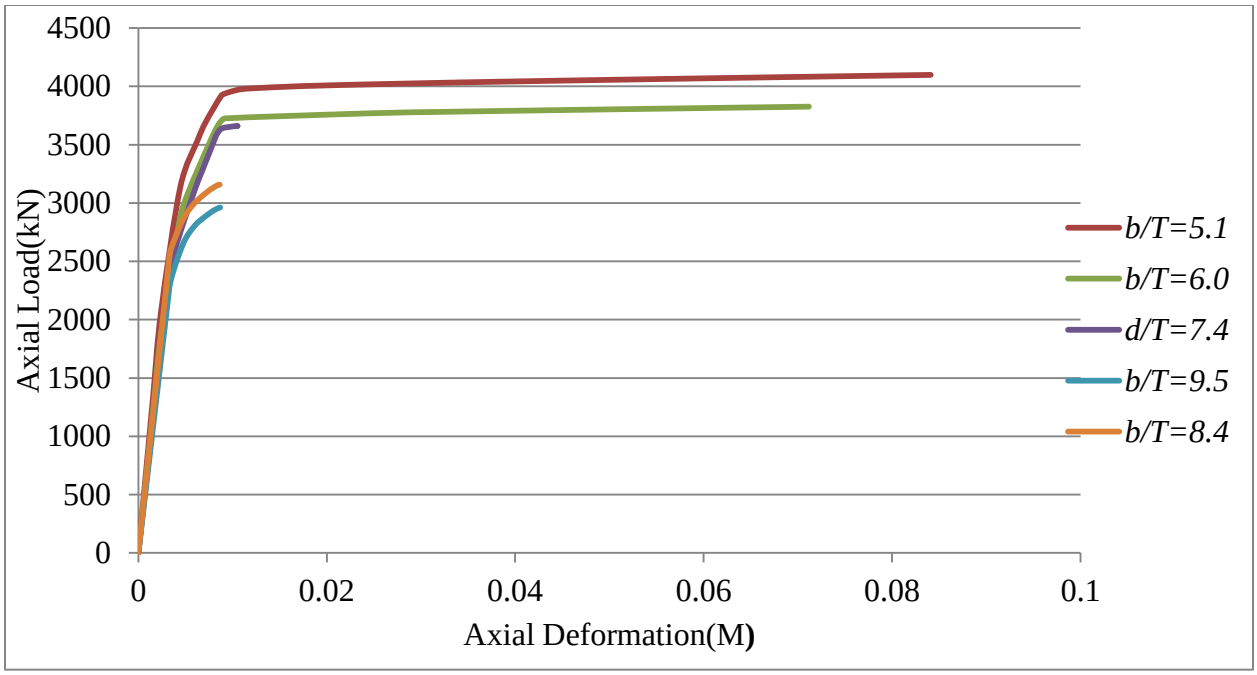

Figure 4.1 Axial load versus axial displacement curve for group one specimens

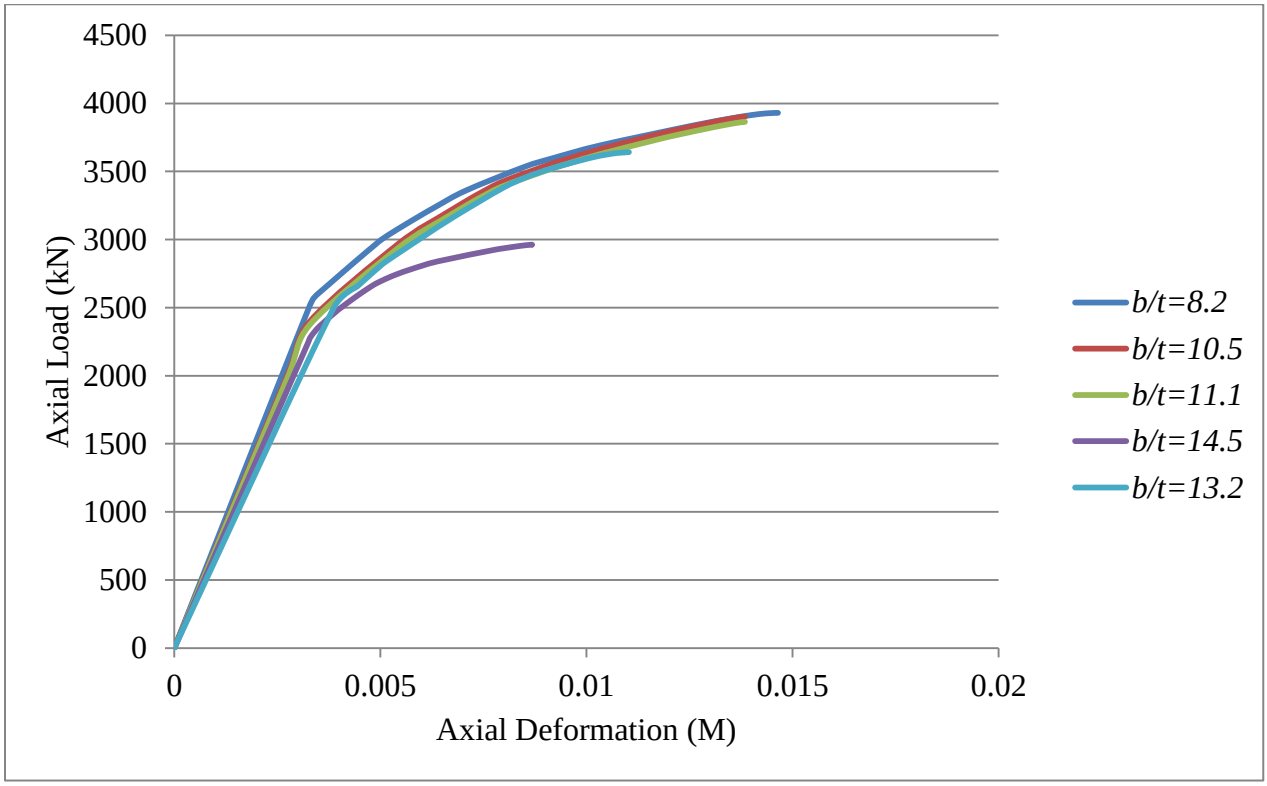

Figure 4.2 Axial load versus axial displacement curve for group two specimens

Table 4.1 Effects of thickness ratio on the peak axial load

Serial number	Specimen	*b/t*	*b/T*	Peak axial load(kN)	Percent difference
GROUP-ONE	C-1	14.521	9.5	2962.33	**Reference**
	C-2	14.521	8.4	3129.552	5.64
	C-3	14.521	7.4	3657.195	23.46
	C-4	14.521	6.0	3826.6842	29.18
	C-5	14.521	5.1	4098.83	38.37
GROUP-TWO	C-6	14.52	9.5	2962.33	**Reference**
	C-7	13.23	9.5	3642.38	22.96
	C-8	11.12	9.5	3864.69	30.46
	C-9	10.45	9.5	3903.34	31.77
	C-10	8.232	9.5	3930.739	32.69

4.1.2. Modes of failure

The failure mechanism of all specimens in this study was concrete crushing combined with yielding of reinforcement which is the same as the failure mechanism of (Tremblay, et al., 1998) and (Chicoine, et al., 2002) of an experimental investigation on the behavior of PEC on stub column under monotonic concentrated load. The point at which the failure marked (highly stressed area) was different with different variables. The influence of width to thickness flange (*b/T*) and width to thickness of web (*b/t*) on the failure mode of PEC is illustrated in Figures 4.3 through 4.9.

When concrete encasement removed yielding of steel flanges and yielding of reinforcement observed as shown in figure 4.5. Ductility of PEC column increases when *b/T* and *b/t* ratio decreases. In specimen C-5 the flange was highly stressed due to lateral expansion of concrete and lack of contact between structural steel and concrete. In addition, at the peak load yielding of the longitudinal rebar occurred which result in crushing of the concrete.

From the damage plasticity model used in this study, tensile cracking and the compressive crushing failure mechanisms were observed. Figure 4.7a shows that the crushing of concrete appeared around mid-height of a column which results in decreasing the carrying capacity of the concrete that causes early failure. It has been observed in Figure 4.9b, concrete around the mid-height of the composite column was cracked due to tensile stress developed in the concrete. But the location of the critical section is different as illustrated in Figures 4.7 and 4.9.

Due to variation of the *b/t* in all specimen of group two concrete in one side of flange experience lateral expansion. Generally, the significant difference on location of the critical section has not been seen in group two specimens when compared with group one specimen. Since the web of the steel section is fully restrained by the concrete encasement while the flange is not supported laterally and highly stressed by the outward expansion of concrete. This indicates that the failure behavior is highly influenced by the *b/T* ratio.

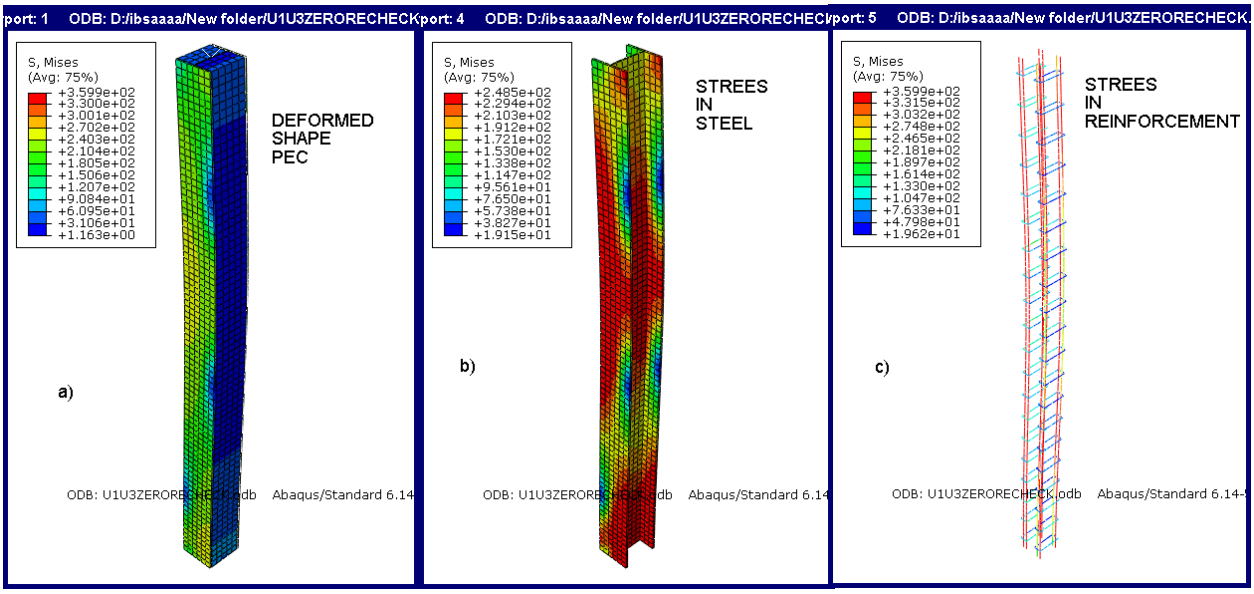

Figure 4.3 Deformed shapes of a specimen C-1

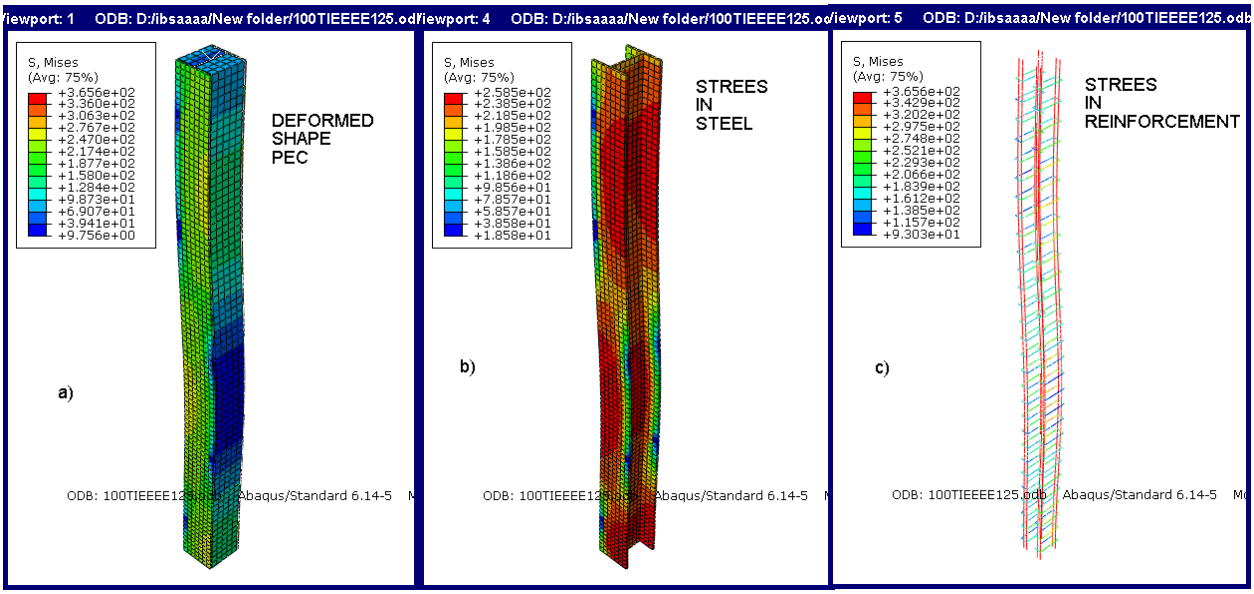

Figure 4.4 Deformed shapes of a specimen C-2

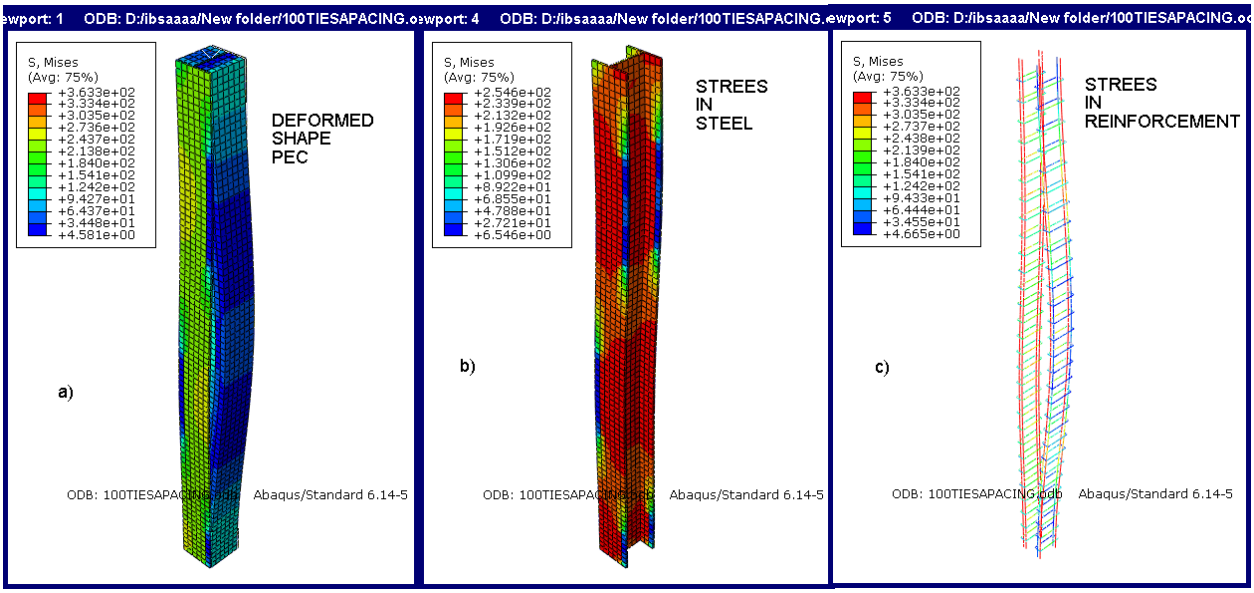

Figure 4. 5 Deformed shapes specimen C-5

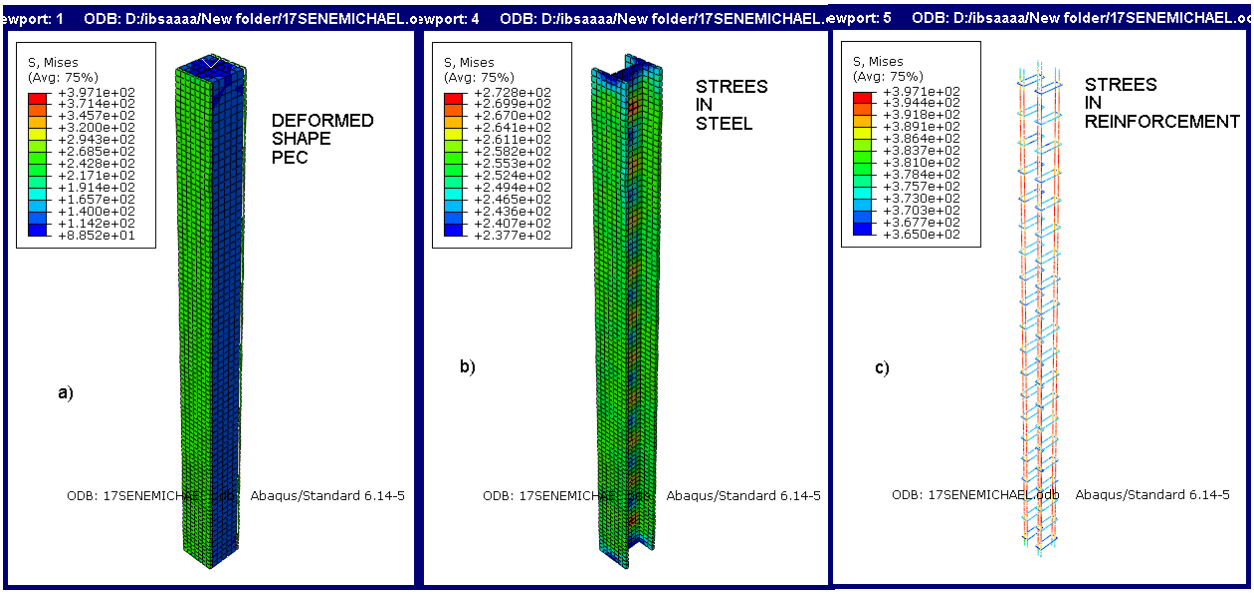

Figure 4.6 Deformed shapes of a specimen C-4

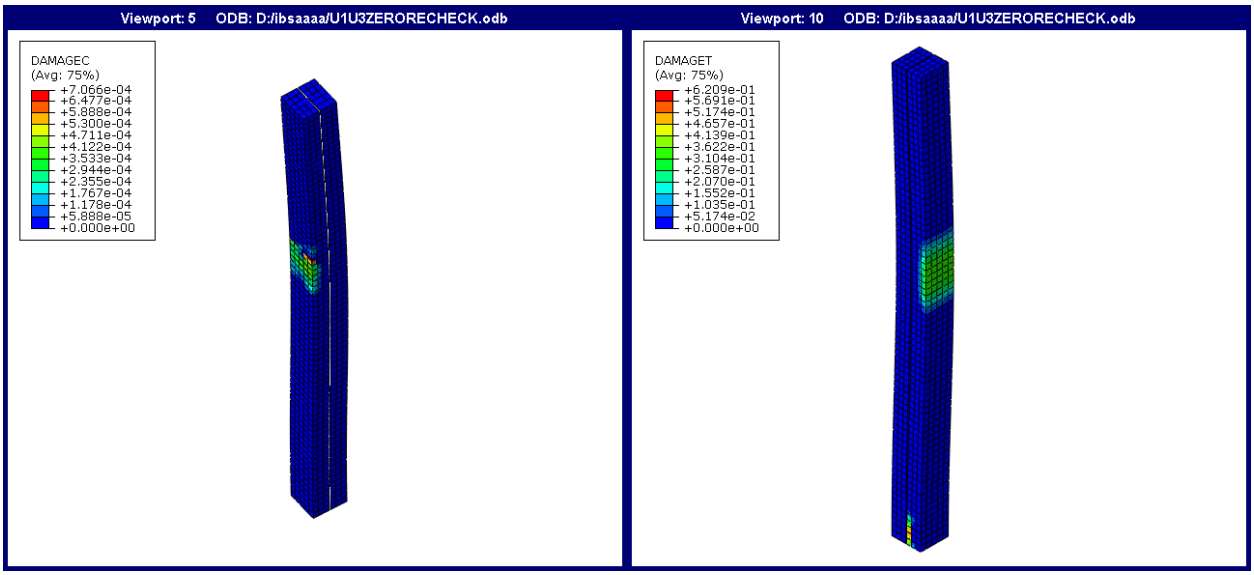

a. compressive damage b. tensile damage

Figure 4.7 Damage of concrete for specimen C-1

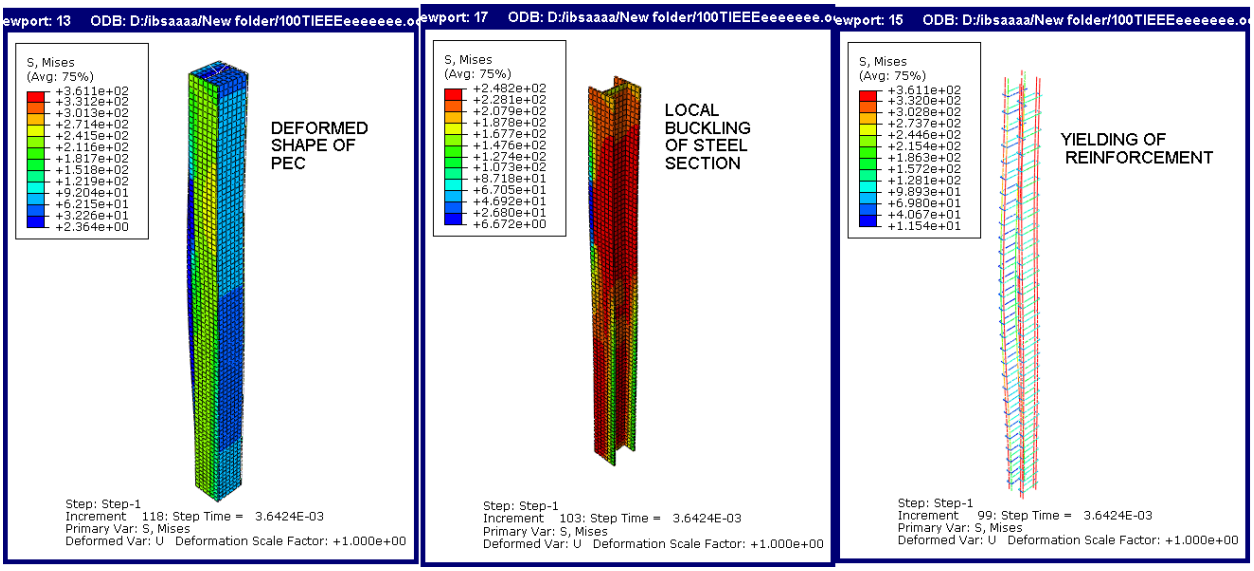

Figure 4.8 Deformed shapes of specimen C-7

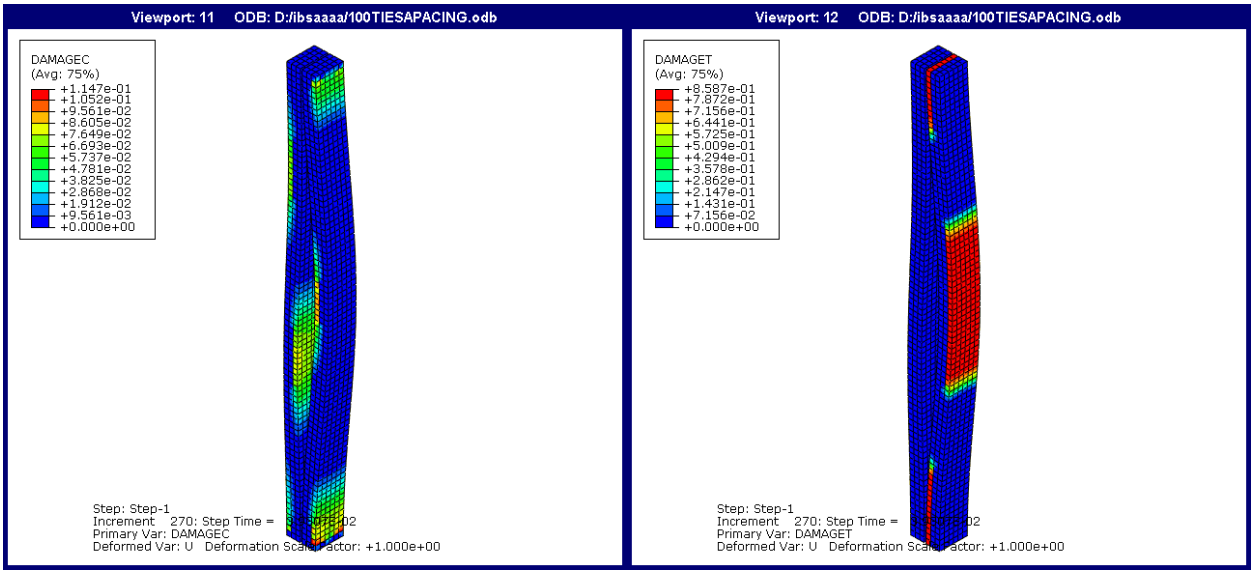

a. compressive damage b. tensile damage

Figure 4.9 Compression and tension damage of specimen C-10

4.2. Effects of link shape on the response of PEC column

The transverse link is provided in between the flange of the H-section to support the free border of the steel flange, to confine concrete, and to control outward deformation of flange and concrete. However, the shape (arrangements) of the transverse link affects the ultimate load-carrying capacity and failure behavior of the PEC column. In this study, three types of link arrangements have been taken (horizontal, X-shape, and Z-shape). The output result from the analysis presented in terms of load-deformation response and failure modes from output stress and concrete damage plasticity. Detail discussion has given in the following section.

4.2.1 Load-deformation response

The influence of links on the response of the PEC column can be according to the link arrangement (shape). Link shape affects the ultimate capacity of the PEC column.

The output result shows that the X- shape link arrangement has a higher ultimate load capacity and shows more ductile behavior than the horizontal and Z- shape links. The peak capacity of the column is higher when we use X-shape and Z-shape link arrangement when compared to the column which is reinforced by longitudinal reinforcement. When comparing C-4 of with specimens C-12 and C-13. The peak capacity of specimen C-4 was 4098.88kN and the peak capacity of C-12 and C-13 were 6340.62kN and 5278.07kN respectively. The difference in percentage of peak axial load of specimen C-4 when compared with C-12 and C-13 were 35% and 16.6% higher respectively. This indicates that the peak capacity of the PEC column significantly increased when the transverse links provided between the flanges specially X and Z shapes.

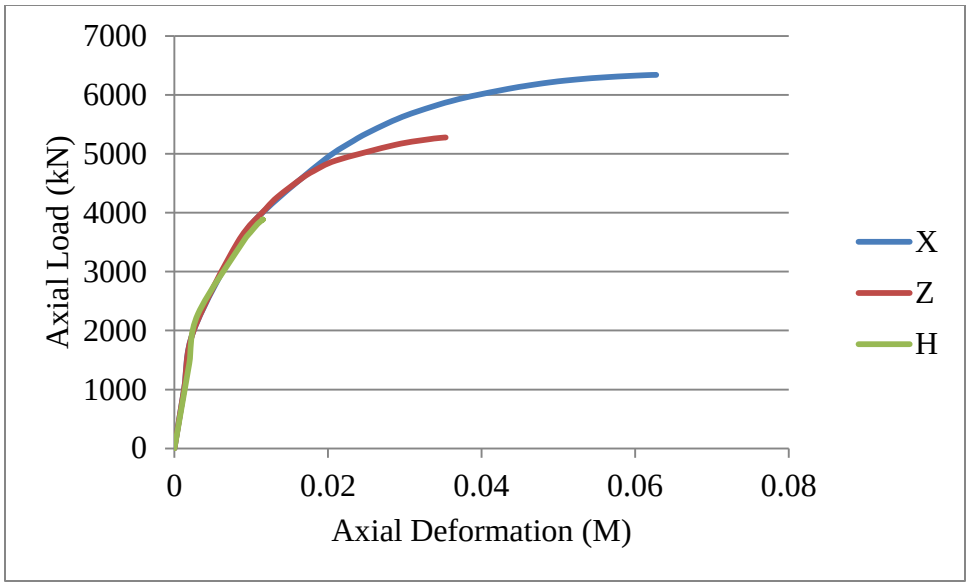

Figure 4.10 Axial loads versus axial deformation for group three specimens

Table 4. 2 Effect of link arrangement on the peak axial load

Serial number	Specimen	Peak axial load (kN)	Percent difference	Link arrangement
GROUP THREE	C-11	3885.52	Reference	H
	C-12	6340.62	38.72	X
	C-13	5278.07	26.38	Z

4.2.2 Modes of failure

The influence of the transverse link on the failure mode of PEC is illustrated in Figures 4.11 through 4.16. The failure in the columns in group three of Table 3.1 was attended by the crushing of concrete combined with yielding of transverse links. The modes of failure were identified by examining the output stress and concrete damaged plasticity model. As it observed from failure mode PEC column in group three specimens there is no lack composite action between concrete steel and links. This indicates the link provide strong confinement to the concrete by minimizing the lateral expansion of concrete, provide lateral support for flange and increase the load capacity of the PEC.

Link provides transverse constrained to concrete and the flanges are less susceptible to local buckling. X-shape link shows more ductile behavior and higher load-carrying capacity than

horizontal and Z-shape links. It has been observed from the output results that concrete failed by crushing as illustrated in Figures 4.14a, and figure 4.15a. But the location of the critical section is different.

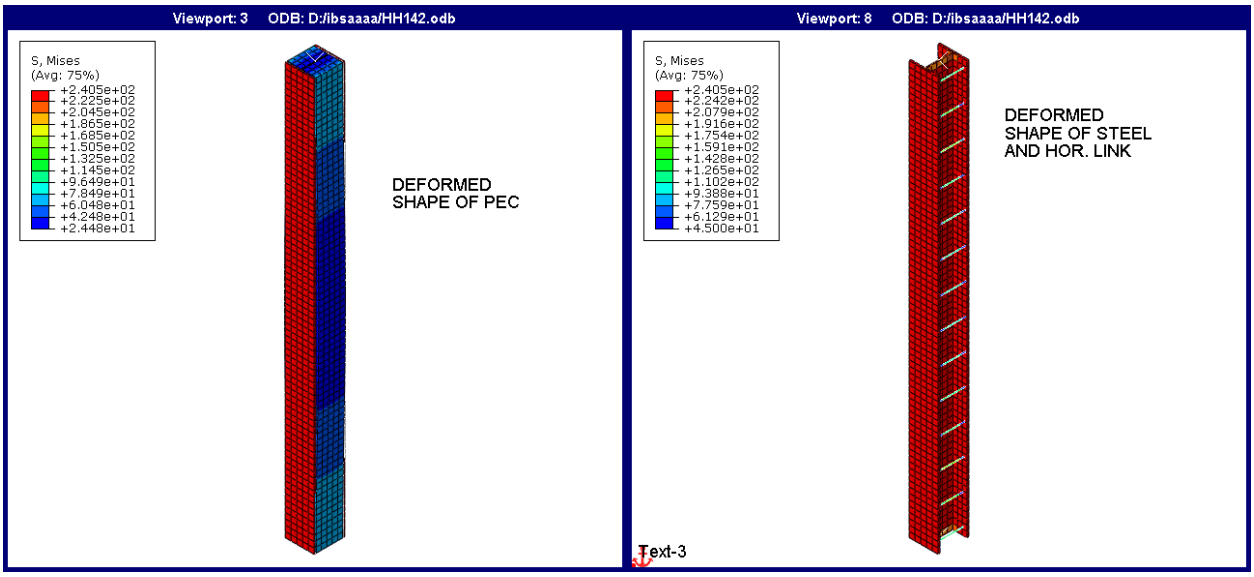

Figure 4.11 Deformed shapes of specimen C-11 with horizontal link

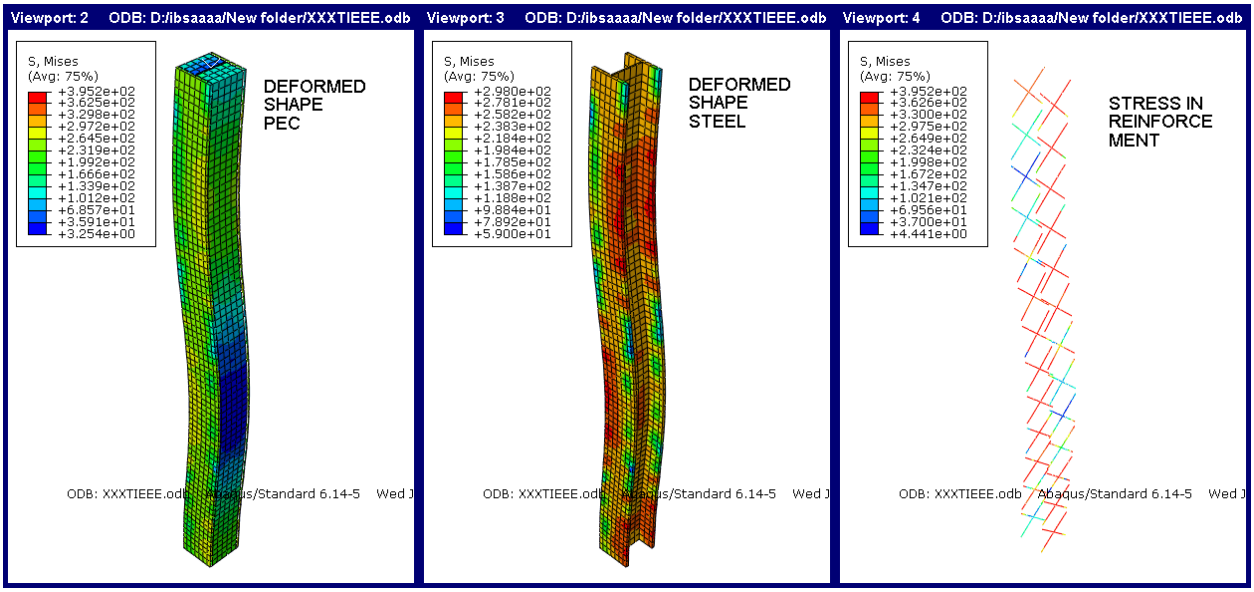

Figure 4.12 Deformed shapes of specimen C-12 with X-shape link

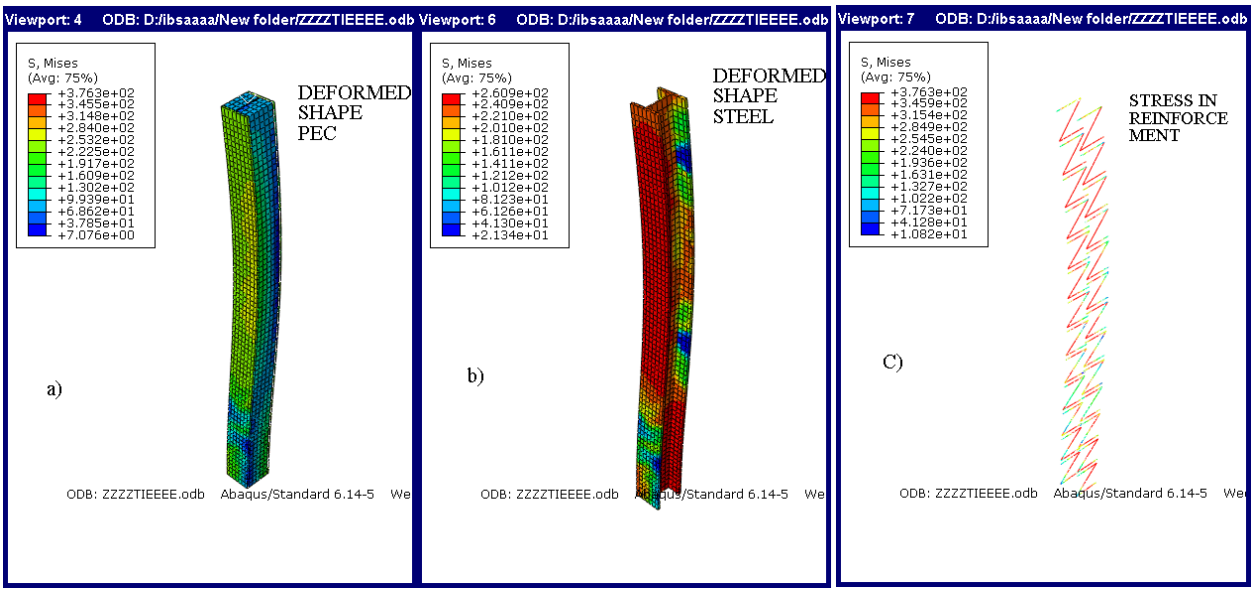

Figure 4.13 Deformed shapes of specimen C-13 with Z-shape link

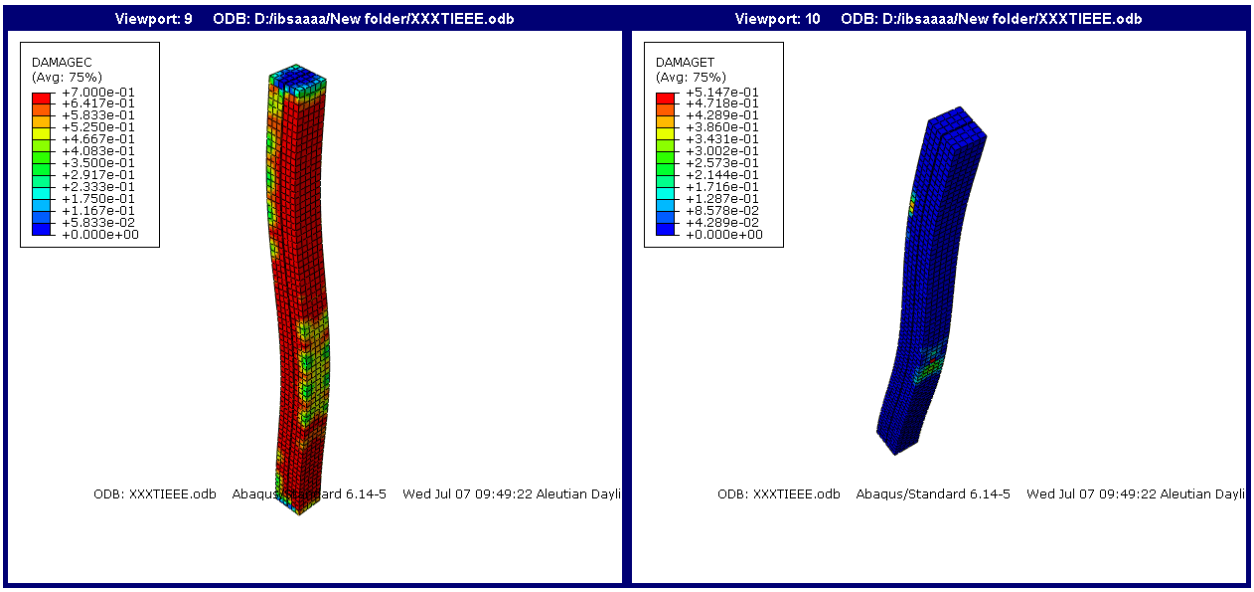

a) Compressive b) tensile damages

Figure 4.14 compression and tension damage of concrete of specimen C-12 with X-shape link

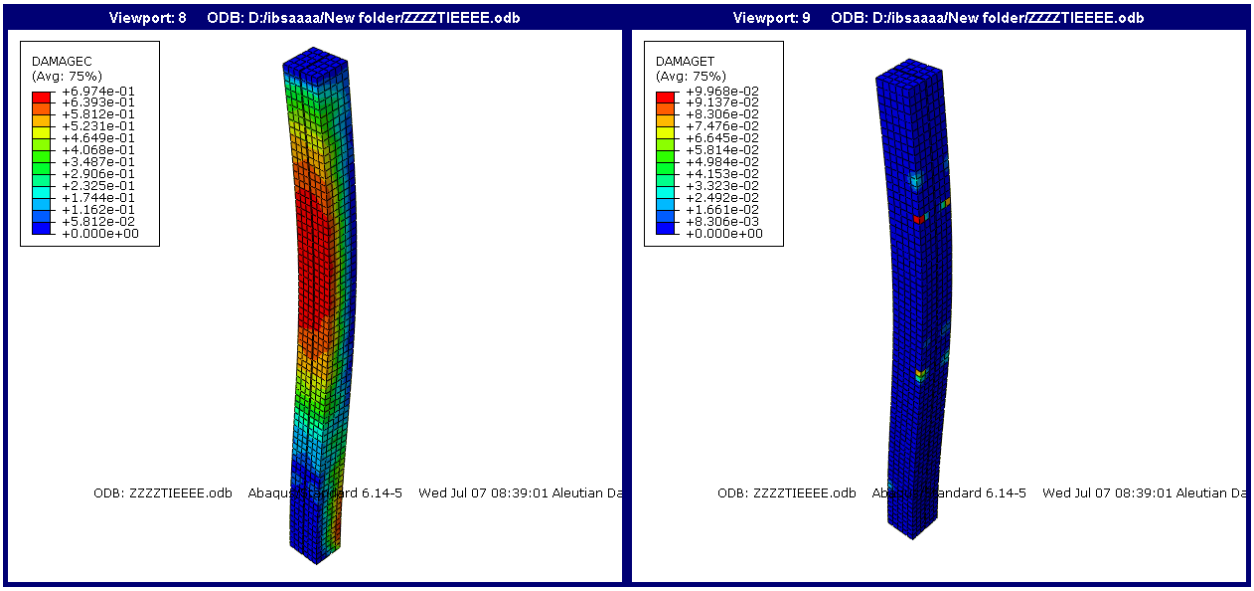

a) Compression damage b) Tensile damage

Figure 4.15 compression and tension damage of concrete of specimen C-13 Z-shape link

CHAPTER FIVE

CONCLUSION AND RECOMMENDATION

5.1 CONCLUSION

This study aimed to investigate the response of the PEC column which is subjected to axial compressive loading. The parametric study was conducted on a series of fourteen specimens. A nonlinear 3-D nonlinear finite element model was developed to model a partially encased composite column. Based on the findings of this study, within the present scope of work and investigation carried out, the following conclusions may be drawn.

The load capacity of PEC columns was increased with the decrease of depth to thickness ratio of flange and width to thickness of the web. The failure mode of partially encased composite columns consists concrete crushing combined with yielding of reinforcement. However, the use of transversal links between the flanges modifies the failure behavior and load capacity by reducing the local buckling of the steel flange and providing confinement to the concrete. From three types of link shape the X-shape link has higher peak load capacity than horizontal and Z-shape links.

5.2 RECOMMENDATION

The following recommendations are made for future investigations.

- The effects of the different loading on the response of composite columns with high-strength materials may be investigated.
- The effects of the thickness of structural steel on the fully encased and in filled composite columns with different loading should be investigated.
- In this study the inclination angle for the X and Z shapes was 45 degrees so, the effects of using another inclination angle should be studied.
- This research is made based on a theoretical basis; the experimental study should be conducted in future works.
- Due to partial concrete encasement, steel flanges are exposed to the environment and vulnerable to fire and corrosion attack which affects the long-term durability of CES columns especially, under extreme conditions. The long-term behavior of PEC under extreme conditions and fire should be studied.

REFERENCES

Anon., 2015. Design equation for the axial capacity of partially encased non-compact columns. *Department of Civil, Geological, and Mining Engineering.*

Begum, M., Driver, R. G. & Elwi, A. E., 2013. The behavior of partially encased composite columns with high strength. *Engineering Structures*, Volume 56, pp. 1718-1727.

Begum, M., Driver, R. G., M.ASCE, A. E. E. & M.ASCE, 2007. Finite-Element Modeling of Partially Encased Composite. *Journal of Structural Engineering*, Volume 133.

Chen, C. C. et al., 1999. *Seismic behavior and strength of concrete-encased steel stub columns and beam-columns in Chinese*, s.l.: Architecture and Building.

Chen, Y., Wang, T., Yang, J. & Zhao, X., 2010. Test and numerical simulation of partially encased composite columns subject to axial and cyclic horizontal loads. *international journal of steel structure*, Volume 10, pp. 385-395.

Chicoine, T., Massicotte, B., Ricles, J. M. & Lu, a. L.-W., 2002. Behavior and Strength of Partially Encased Composite. *Journal of Structural Engineering.*

Chicoine, T., Massicotte, B. & Tremblay, a. R., 2003. Long-Term Behavior and Strength of Partially Encased. *structural engineering.*

Chicoine, T., Tremblay, R., Ricles, B. M. J. M. & Lu, L.-W., 2002. Behavior and Strength of Partially Encased Composite Columns with Built-up Shapes. *Journal of Structural Engineering*, Volume 128, pp. 279-288.

ES EN 1993-1-1, Euro code 3: Design of Steel Structures-Part 1-1. General Rules and Rules for Buildings, 2005

Euro code 4:EN 1994-1-1:2004 Design of composite steel and concrete structures

Cristina, C., Nagy, Z. & Pop, M., 2015. Behavior of Fully Encased Steel-Concrete Composite Columns. *Procedia Engineering.*

Hafezolghorani, M., Hejazi, F., R., V. & S., &. J. M., 2017. Simplified Damage Plasticity Model for Concrete. *Article in Structural Engineering International.*

Han, L. H. A. Y. F. R. C. &. R. Q. X., 2015. Performance of concrete-encased CFST. *Journal of Constructional Steel Research,* Volume 106, pp. 138-153.

Jamkhaneh, M. E., Kafi, M. A. & Kheyroddin, A., 2019. Behavior of partially encased composite members under various load conditions Experimental and analytical models. *Advances in Structural Engineering,* Volume 22(1), pp. 94-111.

Kmiecik, p. & Kamiski, m., 211. modelling of reinforced concrete structures and composite structures with concrete strength degradation taken into consideration. *archives of civil and mechanical engineering,* 11(623-636).

K, P. & Socrates, S., 2019. Study on the Structural Behavior of Concrete Encased Steel Composite Column. *International Research Journal of Engineering and Technology,* Volume 6.

Kwaśniewski, L., Szmigiera, S. & Siennicki, M., 2011. Finite Element Modeling Of Composite. *Archives Of Civil Engineering.*

Lai, B. et al., 2020. Assessment of high-strength concrete encased steel composite columns subject to axial compression. *Journal of Constructional Steel Research,* Volume 164.

Ma, D. Y. et al., 2018. Seismic Performance of Concrete-Encased CFST Piers Analysis.. *Journal of Bridge Engineering,* Volume 23.

Pereira, M. F., Nardin, S. D. & Debs, A. L. E., 2015. Structural behavior of partially encased composite columns under axial loads. *Steel and Composite Structures.*

Portolés, et al., 2013. Simulation and design recommendations of eccentrically loaded slender concrete-filled tubular columns. *Engineering Structures,* Volume 35, pp. 1576-1593.

Rahman, M. S. & Begum, M., 2017. Numerical Simulations of Fully Encased Composite Columns under Gravity Loads. *Applied Mechanics and Materials,* Volume 860, pp. 140-145.

Rahman, M. S., Begum, M. & Ahsan, R., 2016. Comparison between Experimental and Numerical Studies of Fully Encased Composite Columns. *International Journal of Structural and Construction Engineering,* Volume 10.

Song, Y.-C., Wang, R.-P. & Li, J., 2016. Local and post-local buckling behavior of welded steel shapes in. *journal of structural engineering.*

Tremblay, R., Massicotte, B. F. I. & Maranda, R., 1998. Experimental study on the behavior of partially encased composite columns made with light welded H steel shapes under compressive axial loads. *Proceedings of Annual Technical Session, Structural Stability Research Council, Atlanta, GA,* pp. 195-204.

Xianzhong Zhao, F. W.-M. C. S. C., 2019. Theoretical Stress-Strain Model for Concrete steel-Reinforced Concrete Columns. *Journal of Structural.*

Y. M. Hunaiti BSc, M. P. & B. Abdel Fattah, B. M. P., 1994. Design considerations of a partially encased composite column. *Engrs Structs and Bldgs.*

Y. M. Hunaiti, B. M. P. a. B. A. F. B. M. P., 1994. Design considerations of partially encased composite column. *Engrs Structs and Bldgs.*

Zhang, et al., 2011. Experimental Research and Finite Element Analysis of concrete-filled Steel Box Columns with Longitudinal Stiffeners. *Advanced Materials Research,* Volume 287, pp. 1037-1042.

APPENDIX

A. MATERIAL INPUT DATA SHEET FOR ANALYSIS

i. Confined concrete input for CDP Model in ABAQUS CAE

Table A. 1 plasticity parameters

Dilation angle	Eccentricity	f_{bo}/f_{co}	K	Viscosity parameter
36	0.1	1.16	0.667	0

Table A. 2 ABAQUS Compressive behavior input

бc	εin	dc
0	0	0
7.71323	4.9E-06	7.3E-05
13.9669	4.1E-05	0.0006
19.6132	0.00011	0.00168
24.2328	0.00021	0.00332
27.8515	0.00035	0.00557
30.4943	0.00052	0.0085
32.1854	0.00071	0.0122
32.9481	0.00094	0.01674
33	0.00102	0.0185
32.8051	0.00119	0.02222
31.7782	0.00147	0.02872
29.8886	0.00178	0.03631
27.1569	0.00212	0.04505
23.6029	0.00248	0.05501
18.9499	0.0029	0.06696

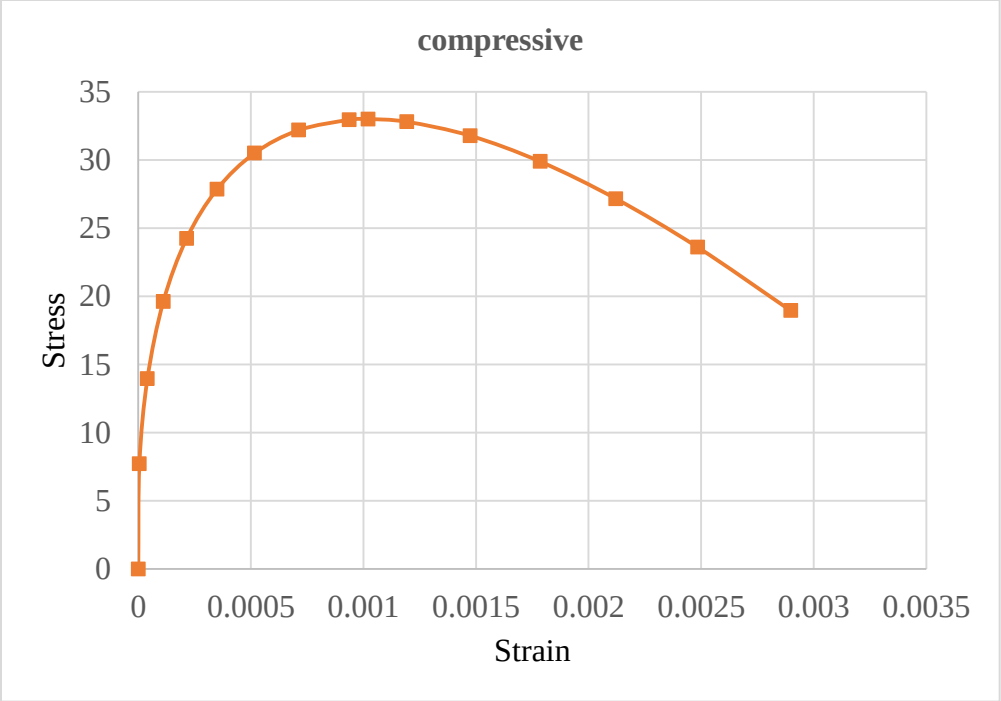

Figure A. 1 compressive concrete input stress-strain curve

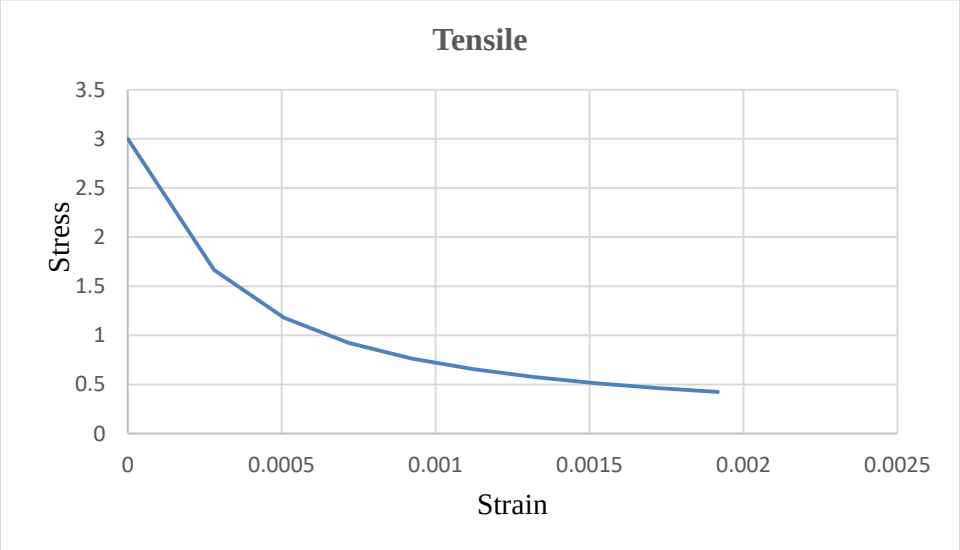

Figure A.2 Stress-crack opening relation for uniaxial tension

Table A. 3 ABAQUS Tension behavior input

δ_t(Mpa)	εin	dt
3	0	0
1.664354	0.000281	0.445215
1.179148	0.000507	0.606951
0.923358	0.000718	0.692214
0.76383	0.000923	0.74539
0.654173	0.001124	0.781942
0.573836	0.001324	0.808721
0.512265	0.001522	0.829245
0.463463	0.00172	0.845512
0.423761	0.001917	0.858746

Table A. 4 Input values for plastic behavior of longitudinal reinforcement

Material type	True stress [mPa]	Plastic strain
Rebar	365.17	0.0023
	591.6	0.08388
Structural steel	235.6	0.0023
	435.6	0.1125

B. OUT PUT FROM ANALYSIS

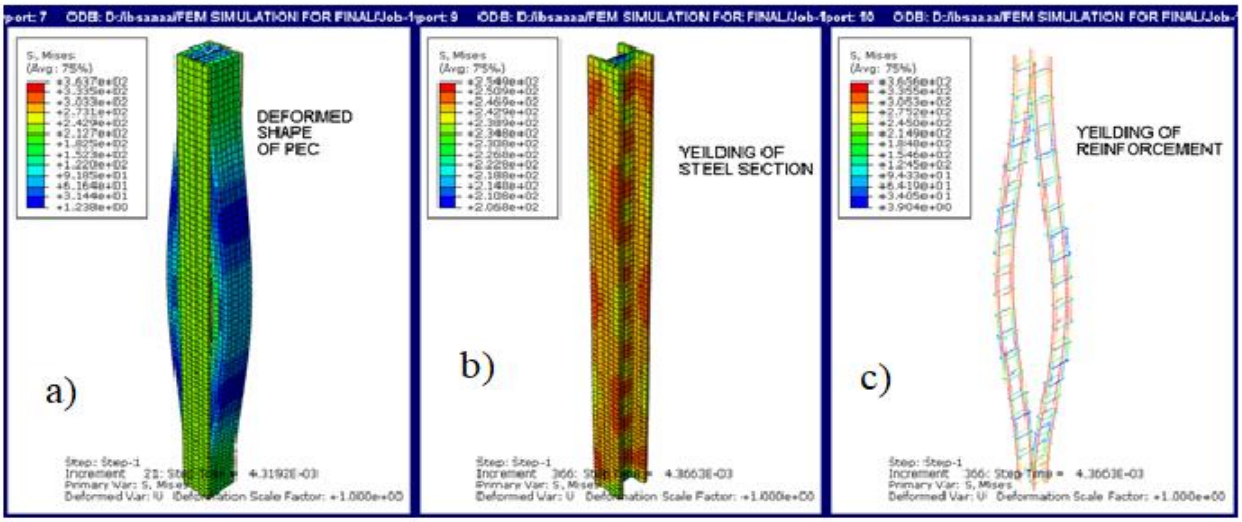

Figure B.1 Deformed shapes of specimen C-5

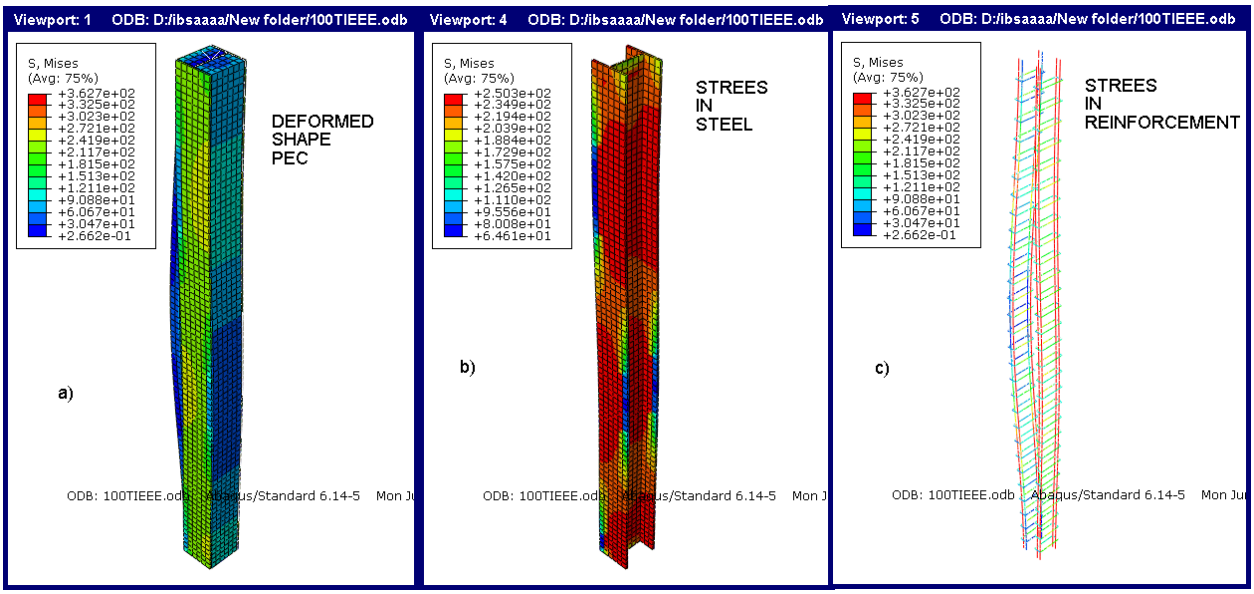

Figure B.2 Deformed shapes of specimen C-8

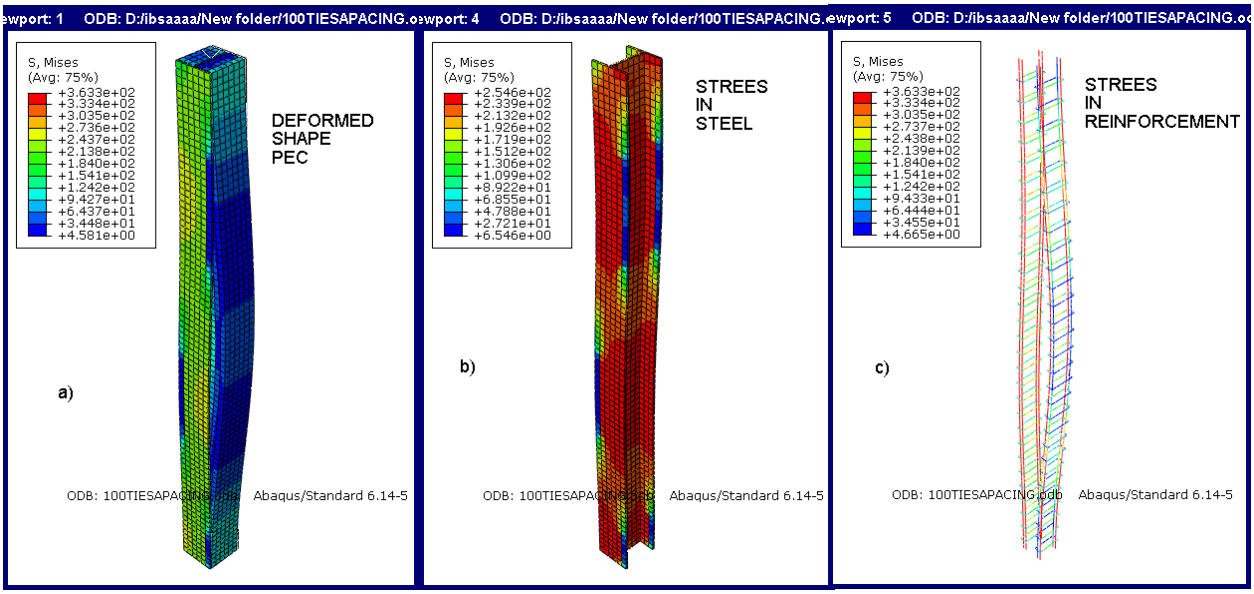

Figure B.3 Deformed shapes of specimen C-10